

A Roadmap for Borophene Gas Sensors

Juan Casanova-Chafer*

Email: juan.casanovachafer@umons.ac.be

Chimie des Interactions Plasma Surface group, Chemistry Department, Université de Mons, 7000 Mons, Belgium.

KEYWORDS: borophene, chemical sensors, gas sensing, superficial oxidation, relative humidity, sonochemical exfoliation, molecular beam epitaxy, chemical vapor deposition, DFT, NEGF

ABSTRACT: Borophene, a two-dimensional allotrope of boron, has emerged as a promising material for gas sensing due to its exceptional electronic properties and high surface reactivity. This review comprehensively overviews borophene synthesis methods, properties, and sensing applications. However, it is crucial to acknowledge the substantial gap between the abundance of theoretical literature and the limited experimental studies. While theoretical investigations have elucidated the stability and remarkable sensing capabilities of various borophene polymorphs across different gases, significant experimental challenges have hindered the translation of these theoretical predictions into practical devices. Consequently, this review carefully studies these challenges and shortcomings that are jeopardizing the practical implementation of borophene in real-world settings. Specifically, four key issues are thoroughly studied such as superficial borophene oxidation upon exposure to the air, interference from relative humidity on gas molecule detection, lack of selectivity, and synthesis scalability. Finally, novel strategies are proposed to overcome these bottlenecks. By adopting these approaches, borophene can pave the way to drive the advancement of the next generation of sensing devices.

Introduction

The rapid expansion of the Internet of Things (IoT), characterized by an extensive network of interconnected devices capable of sensing, collecting, and exchanging data, necessitates a widespread deployment of sensors across varied environments.¹ This scenario highlights the critical demand for cost-effective and scalable sensor technologies.² The affordability of sensors significantly impacts the adoption rate and feasibility of comprehensive IoT solutions, particularly in scenarios necessitating dense sensor networks for detailed data acquisition.³ Furthermore, the trend towards miniaturization of sensor devices, driven by the requirement for integration into diverse environments, emerges as another critical factor.^{4,5} Miniaturized sensors confer numerous benefits, including reduced material consumption, diminished energy requirements, and compatibility with integration into complex systems.⁶ These sensors can be designed to communicate wirelessly with central control systems or other devices, enabling an efficient integration into existing infrastructure.⁷ For example, in urban areas, borophene sensors could be

deployed across a network to continuously monitor air quality levels, detecting pollutants such as nitrogen dioxide, ozone, and particulate matter.^{8,9} The data collected by these sensors can then be analyzed in real-time to reveal the pollution trends and inform authorities and public health institutions for decision-making, such as adjusting traffic flow.

This real-time capability could be further advanced by exploring nanoscale materials with high surface reactivity and smaller dimensions. Despite the attention garnered by carbon-based structures (i.e., carbon nanotubes and graphene) over the past decade for their exceptional sensing capabilities,¹⁰ the limitations of these materials have motivated the scientific community to seek out new types of 2D nanomaterials that can overcome these challenges and enhance overall sensing performance. In this context, boron exhibits potential for fine-tuning its properties for different applications is significant due to boron's lighter atomic weight compared to carbon and its ability to create various chemical bonds.¹¹ Notably, boron nanostructures exhibit versatility in dimensionality, ranging from 0D^{12,13} to 1D¹⁴ and 2D.^{15,16}

In this context, 0D boron nanomaterials, known as boron quantum dots (BQDs), offer high surface-to-volume ratios that enhance their sensitivity to gas molecules. Hao and collaborators produced crystalline BQDs from bulk boron powder, with an average lateral size of 2.46 nm and thickness of 2.81 nm.¹⁷ These BQDs exhibit properties that hold significant potential for gas sensing, including quantum confinement effects and multiple reactive sites, which promote efficient gas adsorption and desorption. However, despite these promising attributes, technical challenges limit their practical implementation. For instance, 0D nanomaterials like BQDs suffer from low stability and face difficulties in forming active films with consistent inter-particle interactions. These issues often lead to variable sensor responses, complicating their use in sensing applications. To address these concerns, the same study incorporated BQDs into a poly(vinylpyrrolidone) (PVP) matrix, effectively stabilizing the boron nanostructures.¹⁷ However, embedding BQDs in a matrix may dilute their unique properties, diminishing their potential benefits. This complexity and the challenges in processing BQDs have likely limited their direct implementation in gas-sensing devices, as evidenced by the lack of reported gas sensors based on BQDs. An alternative approach could involve using BQDs as a doping or decorating element in another semiconducting nanomaterial, such as boron nitride (BN)-decorated ZnO nanoplates for detecting benzene, toluene, ethylbenzene, and xylene (BTEX) gases.¹⁸ Nonetheless, BQDs remain promising for applications beyond gas sensing, such as in photoluminescence studies.¹⁹

Moving to 1D boron structures, including boron nanoribbons (BNRs) and nanowires (BNWs), these nanomaterials provide extended conduction pathways that enhance electron transport when interacting with gas molecules. This characteristic is particularly advantageous for detecting low-concentration gases, as their structure allows for efficient charge transfer.²⁰ In 2004, Xu and collaborators synthesized single-crystal α -tetragonal BNRs by pyrolyzing diborane at 630–750 °C and 200 mTorr in a quartz tube furnace.²¹ These nanoribbons had thicknesses ranging from 15 to 20 nm and widths from 800 to 3200 nm. Later, Zhong and co-authors produced even narrower BNRs, averaging 10.3 nm, through the self-assembly of boron on Ag(110) surfaces.²² However, their use in gas sensing for pollutant detection has yet to be reported. Regarding BNWs, it was reported their growth via the CVD method with

diameters ranging from 20 to 200 nm and lengths of several μm .²³ Besides, BNWs have been synthesized using several methods, such as laser ablation,^{24,25} magnetron sputtering,²⁶ thermo-reduction,²⁷ and CVD.²⁸ This versatility in producing BNWs, linked to its semiconducting behavior, makes them highly promising for developing miniaturized gas sensors.²⁹ However, experimental studies on both, BNWs and BNRs, for gas sensing application remain absent, likely due to the low stability of these 1D boron nanostructures in long-term use.²³ Future research may focus on enhancing the stability of BNWs and BNRs through surface passivation or creating heterostructures with other nanomaterials, similar to advancements made with carbon nanotubes, to improve both sensing performance and stability.

Moving forward to the 3D boron structures, known as bulk boron, offer greater stability and ease of handling than their 0D and 1D counterparts. However, bulk boron is essentially unsuitable for developing sensitive gas sensors due to its low surface area-to-volume ratio, and limited and nonspecific interactions with gases. Nonetheless, compared to 0D, 1D, and 3D structures, during the last years the emergence of two-dimensional (2D) nanomaterials represents a breakthrough in nanotechnology and materials science, revealing materials with unique properties and broad potential for various applications. These nanomaterials, distinguished by their atomic thickness, exhibit unparalleled physical, chemical, and electronic properties that enhance sensor development, properties absent in their bulk counterparts.³⁰⁻³² The sheet-like configuration of 2D nanomaterials, for example, affords the highest surface-to-volume ratio among all material forms, advantageous for catalysis and sensing due to the higher density of active sites and heightened analyte interaction.³³ Additionally, quantum confinement effects and significant anisotropy, coupled with mechanical flexibility and robustness, pave the way for developing wearable and adaptable sensors for various surfaces and settings.³⁴ In this context, borophene has already been employed as a high-performance wearable pressure sensor integrated into a health monitoring system.³⁵

Therefore, numerous research efforts have been focused on developing active 2D nanomaterials for sensing applications. However, various intrinsic limitations and shortcomings still need to be improved in their practical implementation in electronic devices. Despite the potential of materials like graphene, known for its excellent carrier mobility, high chemical stability, and low electronic noise, its zero bandgap poses challenges for direct application in electronic devices.^{36,37} Although this zero bandgap can be overcome through the development of graphene oxide (GO) or reduced GO (rGO), such processes escalate the complexity and cost.³⁸ Transition metal dichalcogenides (TMDs), exemplified by MoS_2 , offer advantages such as a finite bandgap yet confront challenges in commercial deployment due to their low carrier mobility.³⁹ Attempts to mitigate this drawback, such as increasing the operating temperature, may compromise device cost, power consumption, and long-term stability. More recently, boron nitride has been proposed as an alternative 2D nanomaterial,⁴⁰ but faces challenges due to its wide bandgap, complicating its application in electronic devices.⁴¹

Borophene, a single atom layer of boron atoms, has emerged as a promising alternative.^{42,43} This monoelemental nanomaterial, with an electronic configuration of $1s^2 2s^2 2p^1$, can form sp^2 hybridizations similar to graphene.⁴⁴ Boustani's work in the late 1990s on ab initio calculations of boron clusters proposed stable configurations of boron

species, including planar surfaces, nanotubes, and hollow spheres.⁴⁵ However, the synthesis of borophene faced challenges due to the inherent instability of boron sheets,⁴⁶ attributed to unoccupied in-plane sp^2 bonds owing to the three valence electrons. In 2007, Tang *et al.* made a significant contribution by proposing boron sheets wherein atoms are arranged in triangular or hexagonal configurations.⁴⁷ This pioneering approach involves the acceptance of electrons, transitioning from two-center bonding to three-center bonding, thereby enhancing the stability of boron sheets. However, borophene as a 2D nanomaterial was first synthesized in 2015 on a silver substrate under ultra-high-vacuum conditions.⁴⁸

Piazza *et al.* proposed the nomenclature "borophene" for 2D boron nanosheets, drawing an analogy to graphene.⁴⁹ Borophene presents promising attributes for implementation in gas sensing devices, such as massless Dirac fermions and an outstanding Fermi velocity.^{50,51} For instance, borophene could be used to detect toxic gases in industrial settings, where its high sensitivity and rapid response time would be advantageous.⁵² However, unlike bulk boron, borophene theoretically exhibits a metallic behavior,⁵³ independent of its phase such as β_{12} , χ_3 , or in a honeycomb arrangement,^{48,54,55} to cite some. Nevertheless, the unique structure of borophene and its strong B-B bonds highlight its potential, with broad possibilities for property modulation, such as transitioning from metallic to direct bandgap semiconducting behavior under mechanical loading.⁵⁶ These tunable properties offer significant potential for developing advanced gas sensing technology by precisely controlling the borophene electronic properties via band structure.⁵⁷ In that way, researchers can engineer sensors with tailored response characteristics optimized for specific gaseous analytes.

This review aims to provide a comprehensive overview of the current status of borophene gas sensors, covering synthesis methodologies, fundamental characteristics, and recent advancements in theoretical and experimental studies. It also identifies the challenges and shortcomings hindering the realization of borophene-based gas sensors in practical applications, such as their instability under atmospheric conditions, the interference of ambient moisture in the sensing process, and the industrial scalability issues. An outlook is provided on the intrinsic challenges and potential future directions for borophene, aiming to shed light on the inherent limitations and deficiencies jeopardizing their integration into nanoelectronics. This roadmap of challenges and possible solutions will guide researchers and professionals in nanotechnology, materials science, and sensor development in their future endeavors.

Borophene Synthesis and Properties

Synthesis. The complexity of B-B bonds confers notable polymorphism to borophene, allowing boron atoms to arrange themselves into a diverse array of crystal structures.⁴⁸ This characteristic highlights the borophene versatility and opens up extensive possibilities for tailoring its properties to develop high-performance devices. The ability to modulate the properties of borophene through its crystallinity highlights its potential in engineering and device fabrication. Additionally, boron vacancies within these polymorphs further enhance the ability to fine-tune borophene properties, providing a pathway for customizing the electronic, chemical, and physical attributes.⁵⁸ In this perspective, it is noteworthy that a recent study has identified up to 16 boron polymorphs.⁵⁹ However, most theoretical and experimental works have been focused on $2-Pmmn$, β_{12} , χ_3 , and honeycomb borophene (Figure 1). The

2-*Pmmn* phase of borophene displays a corrugated structure, while the β_{12} and χ_3 phases present flat structures lacking vertical undulations but exhibiting unique patterns of periodic boron vacancies. Conversely, freestanding honeycomb borophene resembles it like graphene structural arrangement but exhibits comparatively lower stability owing to the boron electron-deficient nature.⁶⁰ As discussed later, the synthesis pathways can be classified as bottom-up and top-down methods to achieve the different borophene phases. Since each approach leads to unique borophene properties and distinct challenges, Table 1 depicts the main advantages and disadvantages of each synthesis method, identifying the primary challenges for industrial application in gas sensing devices, and potential improvements to overcome these technical bottlenecks. The final column offers potential research directions to address existing limitations and advance borophene's practical use. Further details are discussed in the following sections.

Bottom-up methods. Bottom-up synthesis methods construct borophene atom by atom, typically resulting in nanomaterials of high purity, crystallinity, and low defect density. Based on self-assembly and chemical synthesis, this method offers a high degree of control over nanostructure composition, size, and morphology.

Molecular Beam Epitaxy (MBE). The primary method for borophene synthesis MBE, enabling the deposition of atomic-scale layers onto a metal substrate. This advanced technique allows the controlled synthesis of high-purity and crystallinity with atomic precision. Operating under ultra-high vacuum (UHV) conditions, MBE significantly minimizes the presence of impurities and contaminants, which is crucial for achieving high-quality borophene. The process relies on generating molecular or atomic beams that condense on the substrate, allowing for layer-by-layer growth. Critical to this process is the substrate temperature, thereby affecting the growth modes and borophene quality. MBE facilitates the epitaxial growth of materials with precise thicknesses and crystalline properties through accurate control over the temperature, molecular beam flux, and vacuum conditions.^{61,62}

MBE has been extensively utilized to synthesize borophene on various metal substrates. Notably, the lattice of borophene is significantly influenced by the nature of the metal substrate employed, differentiating it from materials like graphene or boron nitride.⁶⁴ Silver foils are commonly used for synthesizing 2D borophene.⁶⁵⁻⁶⁷ However, researchers have also explored other metals such as copper,⁶⁸ gold,⁶⁹ aluminum,⁵⁴ and iridium⁷⁰ to tailor the borophene properties. These variations in substrate lead to anisotropic metallic behavior in synthesized borophene.⁷¹ Nonetheless, the electron-deficient nature of boron, predisposing it to multicenter bonds, presents challenges in synthesizing these monolayers.⁷²

Furthermore, transitioning from single-layer to multilayered borophene alters properties and enhances processability. In principle, single atomic layers of borophene exhibit poor stability and are prone to rapid oxidation.⁷³ Conversely, bilayer borophene demonstrates increased strength and resistance to oxidation, as evidenced by synthesis on Cu (111) and Ag (111) substrates.^{74,75} This transition highlights the potential for customizing the synthesis of borophene to meet specific application requirements. Figure 2 shows the first report of borophene obtained via the MBE growth over an Ag(111) substrate.⁴⁸ In this study, pure boron was vaporized and deposited at high

temperatures between 450 and 700 °C, achieving deposition rates of 0.01 to 0.1 monolayers per minute. More recently, Li and co-authors studied the effect of the post-annealing process on borophene growth via MBE on Cu(111) substrates.⁷⁶ They observed that boron nanostructures could gradually transition from clusters to striped-phase borophene, representing an intermediate phase that can eventually develop into β -borophene. This approach produced borophene with triangular shapes and with lateral sizes of only a few nanometers. This confined size offers great potential for gas detection. However, technical challenges arise, like poor mechanical stability and difficulties with manipulation and transfer.

However, while MBE is a powerful technique for small-scale or research-oriented projects, its implementation in real-world settings presents inherent challenges. MBE systems are complex and expensive to set up and maintain due to requirements such as high vacuum chambers, metal-oriented substrates, and sophisticated control systems.^{77,78} Additionally, the generation of borophene through MBE occurs at a slow rate, resulting in small quantities of the nanomaterial being produced. This limited scalability hinders its practical application in industrial uses, requiring more significant amounts. Consequently, while MBE offers precise control over few-layer growth and is widely utilized in research, its significant limitations in practical applications must be acknowledged. Despite achieving high quality and crystallinity through the MBE technique, another issue arises with the additional transfer step required for borophene. This transfer step typically results in the deterioration of borophene quality, further constraining its potential application in industrial processes. Consequently, further research is needed to develop new transfer methods and advanced substrate engineering techniques to minimize layer damage during the transfer step. An alternative strategy to mitigate transfer-related risks is the synthesis of large-area borophene. Wu and collaborators successfully produced monolayer borophene sheets up to 100 μm^2 .⁷⁹ However, XPS analysis revealed that 80% of the borophene was oxidized within 1 hour, which limits its practical applications. Nonetheless, from a gas-sensing perspective, smaller borophene sheet sizes would, in principle, enhance sensing performance.

Chemical Vapor Deposition (CVD). This method offers an alternative for depositing thin films of 2D nanomaterials onto substrates through the chemical reactions of precursors. This technique involves the thermal decomposition or reaction of volatile precursors on a heated substrate, forming a solid material as a thin film. The CVD reactor conditions, including temperature, pressure, and precursor gas flow rates, are precisely controlled to customize the deposited material composition, structure, and properties.^{80,81}

Due to CVD high versatility and capability to produce high-quality nanomaterials, significant research efforts have been focused on employing this method to obtain borophene.⁸² Figure 3 shows an example of borophene obtained through this method. Figure 3a-c shows that borophene area sheets are about $5\mu\text{m}^2$, confirmed in Figure 3j, summarizing the area distributions. Besides, Figure 3d-g shows the AFM images and phase diagrams, revealing the high control of the CVD method to obtain monolayer (1L), bilayer (2L), and trilayer (3L) borophene with increasing thickness (Figure 3i-h).⁸³ Furthermore, J. Xu *et al.* successfully produced high crystallinity ultrathin boron sheets of about 10 nm thick on silicon substrates through the thermal decomposition of diborane (B_2H_6).⁸⁴ Figure 3k-l shows scanning electron microscope (SEM) images, revealing the achievement of ultrathin boron

sheets. However, the observed sheet sizes range from approximately 3 to 20 μm in length. This work has paved the way for future obtention of borophene via CVD. More recently, Guo and collaborators used a low-pressure CVD to produce 2D tetragonal borophene sheets on copper foils with a surface area of 1 cm^2 .⁸⁵ These sheets demonstrated an electrical conductivity of approximately 4.5×10^{-4} S/cm and a bandgap of 2.1 eV, making this method promising for semiconductor sensor applications. However, the versatility of borophene opens up additional practical uses. For instance, Tai and collaborators synthesized borophene on carbon cloth using sodium borohydride as the boron source and hydrogen as the carrier.⁸⁶ The resulting α' -borophene exhibited excellent electrocatalytic efficiency for hydrogen evolution (HER).

An interesting advancement in borophene synthesis is the creation of “borophene glass,” closely resembling the theoretical α' -2H-borophene structure.⁸⁷ In this method, NaBH_4 served as the boron source while hydrogen acted as the carrier gas in CVD, depositing borophene directly onto an insulating quartz substrate with a thickness of 3.4 nm. This technique offers the advantage of direct growth on insulating materials, eliminating the need for a transfer step. However, a drawback of CVD is the use of toxic precursors and the potential for hazardous subproduct formation. Addressing this, Jomphoak and co-authors proposed a safer CVD route for borophene synthesis on Cu(111) by replacing the toxic diborane precursor with boron-diborane trioxide.⁸⁸ This approach achieved yields comparable to previous methods, producing borophene layers 3 nm thick with surface areas of approximately $500 \times 300 \text{ nm}^2$.

Nevertheless, many CVD parameters can heavily impact the properties of the resulting borophene. To investigate these effects, Sun and collaborators conducted detailed simulations to understand how precursors like diborane (B_2H_6) decompose on various metal substrates.⁸⁹ Their findings revealed substrate-specific dissociation behaviors, with metals like Pd, Pt, and Rh exhibiting the highest catalytic activity for diborane dissociation, followed by Ir, Ru, and Cu, and lower activity observed in Au and Ag. Among face-centered cubic (fcc) metals, the (100) orientation accelerated B_2H_6 dissociation significantly more than other orientations, paving the way for advanced CVD protocol development.

While CVD methods enable the production of borophene layers with large surface areas and fine control over thickness and phase, the high operating temperatures required often limit the choice of suitable substrates. For industrial scalability, the CVD process also demands precise control over multiple parameters to achieve consistent reproducibility across devices. Flow inhomogeneities within the reaction chamber, for example, can lead to variable results across different regions of the substrate. Nonetheless, CVD remains a promising approach for producing large quantities of borophene and offers a balanced method for both research and practical applications.⁹¹

Top-down methods. This methodology begins with a larger structure, like bulk boron, and is systematically reduced to nano-sized structures through techniques such as exfoliation. The most widely employed method for obtaining borophene is ultrasonication-assisted liquid-phase exfoliation, which has been defined from now on as sonochemical exfoliation.

Sonochemical exfoliation. This technique involves immersing the bulk boron in an appropriate liquid medium and applying high-intensity ultrasonic waves. These waves generate rapid pressure changes in the liquid, leading to the formation and violent collapse of “bubbles”, known as cavitation.^{92,93} Sonochemical exfoliation employs the energy produced by ultrasound waves to promote the intercalation of solvent molecules into the boron layered structures, subsequently exfoliating them into thinner layers or singular sheets by centrifugation (Figure 4a). This method parallels the well-established process of obtaining graphene from graphite.⁹⁴ It is noteworthy that the crystalline structure can be preserved under mild experimental conditions even after sonication, as will be discussed further.

A representative example of this method was performed by H. Li and collaborators, who achieved an industrially scalable synthesis of borophene using sonication-assisted liquid-phase exfoliation, eliminating the need for intermediate chemical reactions.⁹⁰ The authors discovered that the size and thickness of borophene depend on the exfoliating solvent and centrifugation speed employed. Remarkably, dimethylformamide (DMF) proved to be an ideal solvent for obtaining borophene with exceptional stability over 50 days. At the same time, isopropyl alcohol (IPA) enabled the production of borophene with shorter lateral sheet sizes and greater thickness. Additionally, as depicted in Figure 4 b-c, this method eases the production of few-layer borophene sheets with high crystallinity.⁹⁰ More recently, a similar exfoliation approach was employed, incorporating a pre-step based on a solvothermal process. Specifically, bulk boron was initially ball-milled and subsequently subjected to solvothermal treatment in acetone at 200°C before the sonication process, producing borophene with larger lateral sizes and reduced thickness, comprising a few layers of boron.⁹⁵ Similarly, Guo and collaborators produced ultrathin borophene (<2 nm), but intercalating Li ions between the few-layered borophene for energy storage applications.⁹⁶ Although sonochemical exfoliation appears straightforward, numerous parameters can be adjusted to fine-tune the borophene properties. For instance, the addition of neutral poly(ethylene glycol) chains, alongside cationic and anionic surfactants like cetyltrimethylammonium bromide and sodium dodecyl sulfate, enables the engineering of the β -rhombohedral crystal structure in borophene. This approach reportedly yields higher quality borophene with enhanced accessibility of active sites, which shows promise for HER applications and other uses.⁹⁷

In this context, the choice of the exfoliating solvent is of paramount importance in determining the properties of the resulting borophene. Acetone stands out as one of the optimal choices, likely due to its low surface tension, facilitating the exfoliation of bulk boron, and its favorable Hildebrand solubility.^{95,98} Besides, the exfoliation of bulk boron typically exhibits a significant Tyndall effect in a wide variety of solvents. Thus, acetone consistently demonstrates superior suspensions.^{90,95} Additionally, a key parameter is the choice of substrate, for example, the β_{12} phase demonstrates strong interactions with Au(111) substrate. Specifically, the β_{12} phase modulation acts as “strain inducers”, making it particularly promising for flexible and wearable electronics.⁹⁹

Another critical parameter in the sonochemical synthesis of borophene is the centrifugation step. The careful adjustment of the centrifugation speed and time allows for the isolation of borophene with specific size ranges and the attainment of a high prevalence of monolayer, bilayer, or multilayer borophene.⁹⁸ Recently, Najiya and

collaborators produced few-layer borophene by incorporating a pre-sonication hydrothermal process at 180°C for 24 hours.¹⁰⁰ This environmentally friendly method uses water as a reagent, minimizing hazards and reducing the complexity and cost.

This method is facile, cost-effective, and scalable for borophene production. However, a principal limitation of sonochemical exfoliation is the introduction of defects and imperfections due to the subtractive nature of this process. Thereby, this method induces the formation of defects that can significantly alter the physical and chemical properties of the nanostructures. Besides, the defects created during the process likely accelerate the borophene surface oxidation, impacting on the stability. Thereby, further research is needed to enhance the stability of sonochemically synthesized borophene, with strategies such as surface passivation offering potential solutions.

Borophene properties for gas sensing. The exceptional chemical, physical, mechanical, and electrical properties of borophene position it as a promising candidate for integration into a broad spectrum of applications, including catalysis,¹⁰¹ supercapacitors,¹⁰² batteries,¹⁰³ and photodetectors,¹⁰⁴ to cite a few. The unique electronic structure of borophene, characterized by high carrier mobility, excellent thermal conductivity, anisotropic metallic behavior, and optical transparency, holds significant potential for sensor applications.¹⁰⁵ A crucial aspect of electronic devices is the presence of Dirac structures. Since boron is next to carbon in the periodic table, their Dirac cone structures exhibit similarities.¹⁰⁶ Studies on prevalent borophene phases, such as β_{12} ,⁵⁰ and χ_3 ,¹⁰⁷ have highlighted a weak interaction between metal substrates and boron sheets, preserving the Dirac structures. The honeycomb arrangement in borophene can accommodate massless Dirac fermions, leading to properties like high-speed electron transport and potential superconductivity, which are beneficial for high-performance electronic devices.⁵⁰ Indeed, the intrinsic carrier mobility of borophene, as predicted in theoretical studies, surpasses that of graphene at room temperature in specific phases like 8B-*Pmmn*,¹⁰⁸ highlighting its suitability for developing borophene-based sensors.

Additional attributes such as flexibility, strength, and elasticity make borophene an ideal and advanced nanomaterial for flexible electronics. In this sense, Z. Zhang *et al.* reported that borophene has a Föppl-von Kármán value per unit area twice that of graphene, indicating its status as one of the most flexible 2D nanomaterials.¹¹ This flexibility is attributed to the borophene ability to undergo phase transitions under bending and stretching, avoiding strain-induced breakage. Furthermore, the structural polymorphism of borophene exhibits unique mechanical properties, such as a negative Poisson's ratio, high Young's modulus, and excellent critical strain.⁵⁸ Borophene also exhibits additional superior properties, including a more significant Fermi velocity (3.5×10^6 m/s) than graphene,¹⁰⁹ crucial for sensing applications due to its implications on carrier transport and sensitivity towards analytes. Besides, theoretical predictions indicate that borophene may outperform graphene in critical properties like Young's modulus along the armchair direction (574.61 N/m versus 338.08 N/m),¹¹⁰ which is key in flexible sensors. However, it is worth mentioning that the presence of boron vacancy defects can reduce the Young's modulus along this direction, while its impact is almost negligible in other directions, such as the zigzag.¹¹¹ It should also be noted that Young's modulus decreases with temperature.¹¹²

The most frequent borophene phases are anisotropic B₁₂ with parallel ridges and X₃ isotropic hexagonally bonded. Nevertheless, the borophene instability through obtention via different synthesis methods is worth noting. Nonetheless, honeycomb borophene exhibits enhanced stability when grown on a metal substrate. This can be attributed to the metal substrate capability to provide electrons, thus offsetting boron's intrinsic electron deficiency.⁵⁴

Beyond flexible electronics, the borophene potential in transistor applications has also been explored. Despite its theoretical metallic behavior and associated challenges like low stability, the versatility of borophene allows for engineering semiconductor sheets. For example, C. Hou *et al.* synthesized hydrogenated borophene (borophane) with high stability and excellent electronic properties through the thermal decomposition of NaBH₄ under hydrogen.¹¹³

Borophene Gas Sensors

Theoretical studies. To estimate the potential sensing performance of borophene, researchers often employ a combination of *ab initio* density functional theory (DFT) calculations and non-equilibrium Green's function (NEGF) methods. DFT is a quantum mechanical modeling method

of nanomaterials and providing information about the reaction energies. This method iteratively deduces the electron density that minimizes the system's total energy.^{123,124} NEGF elucidates quantum transport in non-equilibrium systems, such as electronic devices under bias voltage, revealing the potential current-voltage relationships, conductance, and density of states, making it indispensable for semiconductor device analysis.^{125,126} The synergy of DFT and NEGF is an effective framework for predicting and understanding the properties of borophene and its derivatives.

Pristine Borophene. In this perspective, the interaction between gas analytes and the borophene surface is crucial for determining its gas detection capabilities. Theoretical investigations have substantiated the feasibility of borophene as a sensor material, demonstrating its superiority over other 2D nanomaterials like graphene and MoS₂ in terms of binding energies and charge transfers.⁵³ The nature of the interaction between borophene and gas compounds is the first consideration when assessing its potential as a gas sensor. Certain gases, including NO₂, NO, CO, and NH₃, are generally chemisorbed on the borophene surface, exhibiting higher adsorption energies (E_{ad}) and a greater detection

capability for these compounds (Table 2 and Table 3). Conversely, gases like CO₂ tend to be physisorbed on the borophene surface, leading to weaker interactions and, thus, lower sensitivity compared to chemisorbed species.¹²⁷ This differentiation between chemisorption and

physisorption has been observed across various crystalline phases of borophene, such as χ_3 ,¹²⁸ β_{12} ,¹²⁹ β_{35} ,¹³⁰ and the hexagonal honeycomb lattice.¹³¹ Figure 5 shows interesting predictions on how five air pollutants would interact with a relaxed unit cell of borophene with lattice constants (a , b) as 1.64 x 2.90 Å.⁵³ Despite CO and CO₂ presenting a bond C-B, while NO, NO₂, and NH₃ show a bond N-B, the shortest bonding distance is similar. Conversely, the N-B presents higher binding energies than the C-O bonds.

The elucidation of charge transfer dynamics between analytes and borophene is crucial in understanding its sensing capabilities. Significantly, the magnitude of charge transfer directly correlates with the potential sensor ability to generate discernible signals, such as variations in resistivity and conductivity. Consequently, higher charge transfers would lead to enhanced sensor responses and lower detection and quantification limits. In this context, Table 2 shows that gases exhibiting weak bonding (physisorption), such as CO₂, demonstrate a minimal charge transfer of -0.09 e (Bader charge), revealing the poor interaction with the borophene surface.⁵³ In contrast, species undergoing chemisorption at the borophene interface involve substantially higher charge transfers, indicative of a stronger interaction and higher adsorption energies.

A detailed examination of the data presented in Tables 2 and 3, corresponding to electron-withdrawing and electron-donating species, unveils significant disparities in charge transfer values. Predominantly, electron acceptor gases exhibit higher charge transfer values than electron donors. This phenomenon might be attributed to the borophene p-type semiconductor behavior, characterized by an inherent lack of electrons, which promotes withdrawing electrons from gaseous molecules rather than donating them. Among the electron-withdrawing species analyzed, NO₂ stands out with the highest energy binding and charge transfer values for pure borophene, positioning it as a potential candidate for developing NO₂ gas sensors. The research conducted by S. Sabokdast and N. Salami also provides an insightful evaluation of the sensing performance of χ_3 borophene nanosheets for various gases, drawing attention to the strong interactions with NO_x gases. However, as a trade-off, these interactions can compromise the sensor recovery and reusability.¹³² These strong interactions, particularly under mild experimental conditions such as ambient temperature operation and low flow rates, may be irreversible or only partially reversible. Consequently, this can compromise the stability and repeatability, alongside inducing issues like baseline drift. To avoid these challenges, strategies such as elevating operating temperatures,¹³³ employing UV light,¹³⁴ or utilizing vacuum pumps¹³⁵ can disrupt these strong interactions and makes easier the release of adsorbed gas molecules, thus cleaning the sensor surface.

Exploratory studies into borophene capacity to detect a broad spectrum of compounds have yielded promising advances. For instance, the sensitivity of β_{36} sheets towards hydrogen cyanide (HCN) unveiled that the borophene unique planar structure, characterized by a central hexagonal vacancy, undergoes significant electronic property alterations upon HCN adsorption, mainly when the molecule binds at the edge of the sheet.¹¹⁹ Furthermore, Q. Sun *et al.* reported the adsorption behavior of several organic molecules on β_1 borophene. Combining DFT and NEGF methodologies, it was identified that molecules like CH₄, CH₃OH, and C₆H₆ undergo physical adsorption. In contrast, HCHO and HCOOH are subject to chemical adsorption, with some inducing a shift in carbon atoms in these organic molecules to sp³ hybridization due to the strong interactions.¹²⁰ This alteration enhances the sensitivity of β_1 borophene to particular analytes and its thermal stability. Interestingly, this study also showed the potential for sensitivity enhancement through mechanical means, such as applying in-plane strain or employing a WS₂ substrate. Similar enhancements were observed when WSe₂ was used as a substrate, forming a van der Waals heterostructure with χ_3 borophene, thereby increasing the nanomaterial stability and sensing performance.¹²⁸

N.N. Hieu *et al.* investigated the impact of gas molecule adsorption on the magnetic properties of monolayer β_{12} borophene.¹³⁶ Despite borophene is hosting Dirac and triplet fermions, it was found that the adsorption of gas molecules on individual boron atoms elicits unique magnetic responses. The intrinsic magnetic properties of pristine borophene are primarily preserved, even with adsorption across multiple boron atoms. However, the study of Pauli spin paramagnetic susceptibility revealed that central atoms in borophene sheets present the highest susceptibility at intermediate thermal energies.¹³⁶

Regarding the total density of states (DOS), theoretical investigations have demonstrated that a pristine borophene monolayer exhibits metallic behavior characterized by the absence of a band gap.⁵³ This intrinsic property significantly influences the interaction between borophene and various gas compounds, particularly those capable of inducing substantial charge transfer in the DOS around the Fermi level. Notably, interactions with a paramagnetic gas, such as NO_2 , result in the hybridization of NO_2 states below the Fermi level with boron p states, transitioning to a nonmagnetic state upon adsorption.⁵³ Further exploration by W. Li *et al.* employing DFT has explored the adsorption capabilities of borophene for various volatile organic compounds (VOCs).¹¹⁷ Their findings reveal that χ_3 and β_{12} borophene can chemically adsorb substances such as ethylene and formaldehyde, releasing significant energy. In contrast, other VOCs, including ethane, methanol, formic acid, methyl chloride, benzene, and toluene, exhibit predominantly physical adsorption, characterized by weaker interactions. Importantly, DOS analysis indicates that chemical adsorption induces modifications in the conductivity of borophene, unlike physical adsorption, which appears to have minimal impact on conductivity.¹¹⁷

Beyond DFT and NEGF methods, F. Zergani and Z. Tavangar used the Climbing Image-Nudged Elastic Band (CI-NEB) method to further elucidate the gas adsorption mechanisms. This work revealed that chemisorbed species, particularly those involving nitrogen or sulfur, may form covalent bonds, as evidenced by analyses of charge density difference and electron localization function.¹³⁷ Additionally, N. Dutta *et al.* have investigated the potential of β_{12} borophene as a field-effect transistor (FET)-based gas sensor, noting significant changes in the energy band structure and density of states upon gas adsorption. This includes the appearance of distinct Van Hove singularities, with a marked increase in carrier concentration for NH_3 and substantial modifications in quantum capacitance and I–V relations, revealing the orientation-dependent nature of NH_3 adsorption.¹³⁸

The application of NEGF methods has revealed that borophene monolayers exhibit anisotropic transport, leading to ohmic behavior.¹³⁹ Calculating the transport properties and corresponding current-voltage functions before and after the gas adsorption can shed light on the sensing performance of resistive or conductance measurements. However, defects are generally considered detrimental in fields requiring highly crystalline samples, such as solar cells. From a gas sensing perspective, the presence of structural defects in borophene, to some extent, can be beneficial in enhancing the interactions with gas compounds. This is attributed to the remarkably low energy defect formation of borophene structures, facilitating stronger adsorption of nitrogen-containing gases like NO_2 and NH_3 at defect sites, thereby acting as reactive sites that increase adsorption energy and charge transfer.¹⁴⁰

Doped Borophene. Doping borophene is a common approach to enhance its electronic, chemical, and physical attributes, aiming to increase its interaction with gas molecules. This approach entails the incorporation of impurity atoms, known as dopants, into the borophene lattice, which can significantly modify its band structure, work function, and surface reactivity.^{141–143} Common methodologies for doping 2D nanomaterials, such as borophene, include CVD, plasma treatments, and electrochemical doping.¹⁴⁴ Moreover, each doping technique presents unique advantages regarding control, uniformity, and scalability, making the selection of a doping method contingent upon the specific application requirements. However, despite the great potential of doping borophene to tailor its interactions with gas compounds, it introduces challenges such as preserving the stability of sheets, managing the distribution of dopants and concentration, and preventing the introduction of undesirable impurities or defects that could compromise the sensing performance. Consequently, selecting an appropriate dopant is imperative to achieve the intended modifications in properties while ensuring the borophene durability in practical applications.

To date, most of the doped borophene used for sensing purposes has been based on theoretical studies. In this perspective, carbon, nitrogen, and oxygen emerge as commonly utilized doping elements, primarily due to their compatibility with plasma functionalization techniques. X. Quin *et al.* elucidated the impact of these dopants on the sensing of various gases, indicating that dopants notably enhance gas molecule chemisorption, especially at the borophene lattice valley bottom B-B bonds.¹²⁷ Thus, borophene doped with elements such as C, N, and O would lead to stronger interactions with gas compounds compared to pristine borophene. Further investigations by N. Hassani and M. Mehdizale into β_{36} borophene doped with transition metals (Fe, Ni, Cu) have demonstrated that metal doping can ameliorate electronic and chemical properties.¹⁴⁵ Nevertheless, according to this study, the sensing efficacy can be notably increased by substituting boron atoms with nitrogen, enhancing the sensing performance through borophene doping and subsequent decoration.

Introducing dopants also transforms the interaction between borophene and target gases, enhancing charge transfer and binding energy. V. Arefi *et al.* conducted DFT studies on pure and sodium-doped borophene for CO and CO₂ detection, discovering that sodium incorporation shifts CO₂ adsorption from physical to chemical (Table 2), markedly improving sensitivity towards this gas.¹¹⁵ Furthermore, I-V curve analyses in this study revealed that sodium doping alters the electrical response of borophene to these gases, with a constant current at a 1.4 V bias voltage, offering a potential mechanism for distinguishing between CO and CO₂. Similarly, X. Tu *et al.* comparison of pure and lithium-doped borophene for SO₂ detection revealed that lithium doping significantly improves the adsorption capabilities of this gas.¹¹⁶ Besides, Li induces a change in the type of interaction, from weak physical to strong chemisorption. However, it is worth noting that high temperatures are required for SO₂ desorption, which can be a potential drawback for gas sensing applications. However, an alternative use of Li-doped borophene can be as a scavenger for SO₂ removal in environmental remediation technologies.¹¹⁶

Additionally, S. Kumar and co-workers have predicted that embedding transition metals into the borophene lattice enhances gas adsorption and confers magnetic properties to borophene, thereby paving the way for its application

in gas sensors and spintronic devices.¹⁴⁶ These multifaceted approaches to doping borophene highlight its versatility and potential in advancing the development of highly sensitive and selective gas sensing technologies.

Borophene Heterostructures. Developing composites from 2D nanomaterials often includes the decoration with metal or metal oxide nanoparticles (NPs) to improve their sensing capabilities. In this sense, J. Anversa *et al.* have made significant contributions by predicting interactions of air pollutants with β_{12} borophene decorated with platinum NPs.¹⁴⁷ Their research demonstrates that platinum preferentially adsorbs at the centers of hexagons on the β_{12} borophene. Thus, its metallic properties were enhanced by introducing new electronic levels, notably 2 eV above the Fermi level, without altering the intrinsic metallic nature of borophene. This arrangement leads to a pronounced charge transfer from borophene to platinum, with a particularly strong interaction with molecules like NO₂ and SO₂. In contrast, interactions with CO₂ molecules remain weaker due to van der Waals forces.¹⁴⁷ These findings, translated to real applications, mean that except CO₂, other molecules such as NO₂ probably require high temperatures to overcome the strong adsorption energy and recover the sensor baseline.

Apart from the pure and decorated borophene, further studies have explored heterostructures such as borophene/boron nitride¹⁴⁸ and borophene/ MoS₂,¹¹⁴ revealing that many chemisorbed gases increase their interaction with the sensor surface. It is worth noting that the NO compound duplicates the charge transfer compared to the pure borophene, as depicted in Table 2. Conversely, CO₂ gas, which presents a weaker interaction, is still physisorbed on the composite despite incorporating additional elements like MoS₂ and boron nitride. This reveals that introducing additional 2D elements can significantly improve the sensing performance towards specific gases, whereas other compounds, such as CO₂, do not benefit from the presence of new elements. This can be a potential tool to improve the selectivity to some extent. Indeed, combining different nanomaterials can significantly impact their sensing properties. For instance, J. Li *et al.* also examined a borophene-MoS₂ composite, but in this case, the borophene is situated on top of a MoS₂ substrate. As a result, the β_{12} borophene on MoS₂ exhibits a pronounced anisotropic gas sensing performance, particularly for NH₃, with an anisotropic gas sensing ratio of 17.43.¹⁴⁹ Moreover, Y. Tian *et al.* also studied the potential sensing capabilities of borophene on a MoS₂ substrate, but further enhanced with gold electrodes for modulating the transport characteristics of borophene.¹⁵⁰ According to these authors, the presence of a MoS₂ substrate introduces non-linearities in the current-voltage behavior. At the same time, gold electrodes tend to donate charges to borophene, creating a potential barrier that lowers the current compared to systems lacking gold electrodes. This parameter presents significant importance for future device design to optimize the transport properties of the borophene nanostructures.¹⁵⁰

Concerning the detection of formaldehyde (HCOH), DFT calculations suggest that certain borophene polymorphs, such as β_{36} , could potentially serve as detectors.¹⁵¹ However, developing a heterostructure by combining SnO₂ with β_{12} borophene markedly improves sensitivity and selectivity towards HCOH, demonstrating the potential of engineering composites for enhanced sensing performance.¹²² According to F. Opoku and P.P. Govender, hybridizing the wide direct band-gap SnO₂ and the metallic β_{12} borophene creates a heterostructure with a moderate direct band gap of 1.09 eV, enhancing the sensing performance. Indeed, HCHO chemisorption can occur in several

orientations on the β_{12} -borophene/SnO₂ surface, acting alternately as a charge acceptor and donor. Not limited to this, the introduction of biaxial strain and an external electric field further improves the system stability, band gap, and charge transfer properties.¹²²

C.-B. Wang *et al.* employed DFT to investigate the adsorption properties of borophene towards several gases, identifying a high adsorption capacity, particularly for nitrogenous gases.¹⁵² According to the findings of these authors, pure borophene presents a potential structural instability upon the adsorption of nitrogenated compounds. Thereby, further stabilization and enhancement of adsorption capacity through a heterostructure of borophene and graphene decorated with lithium were explored, revealing a significant improvement in the adsorption capacity of H₂S. Besides, NEGF studies simulated the transport properties of the composite, suggesting that it can mitigate the borophene deformation during the gas adsorption process.¹⁵²

Further theoretical analyses have also examined the interaction of composite materials with various organic molecules, revealing that the heterostructure composed of borophene and graphene (B/G) displays weak physical adsorption interactions with organic molecules.¹²¹ However, doping the B/G with transition metals may significantly improve chemical interactions by altering the hybridization of carbon atom orbitals. This is especially notable for detecting C₂H₂ even at low bias voltages.¹²¹ In another study, J. Shen *et al.* explored a 2D van der Waals heterostructure composed of borophene and semiconducting 2H-MoS₂ to detect the same organic molecules.¹¹⁸ Their findings correlate with the previous works, demonstrating similar physical and chemical interactions with organic gas compounds. However, the main difference lies in formaldehyde, which exhibits an 8.5-fold increase in charge transfer when using 2H-MoS₂/borophene compared to other works reporting pure borophene. This study also confirms that strong chemisorption, related to a change in the hybridization of carbon atoms to sp³, occurs even at low bias voltages.¹¹⁸

These approaches, comprising the development of borophene-based heterostructures and doped borophene, pave the way for achieving gas sensors with superior sensitivity and selectivity. However, it is worth mentioning that these strategies may lead to greater complexity and higher costs in obtaining the desired nanomaterials. Therefore, evaluating cost-effectiveness is highly recommended before implementing them in commercial devices.

Other Boron-based Nanostructures. Exploring alternative boron-based nanostructures offers promising avenues for tailoring the sensing properties of materials. B. Peng *et al.* studied the potential of β_{40} fullerene for NH₃ detection, theorizing strong chemisorption (up to -1.09 eV), significantly higher than those for other non-polar gases such as H₂, CH₄, and N₂, which tend to be physisorbed. Consequently, it can be expected to discriminate and detect NH₃ when mixed with other non-polar compounds.¹⁵³ M. Fazilaty *et al.* combined DFT and NEGF analyses to investigate H₂S molecule adsorption on χ_3 -borophene nanoribbons. Their findings reveal that H₂S adsorption significantly changes the DOS, transmission spectrum, and I-V curve, indicating partial charge transfer to the χ_3 -borophene.¹⁵⁴

Experimental studies. Experimentally, borophene has been identified as a p-type semiconductor, characterized by holes as the majority of charge carriers.¹⁵⁵ Boron, with one fewer valence electron than carbon, introduces acceptor states into the valence band, which increases the density of states in this region. This leads to p-type conductivity and a narrower bandgap.¹⁵⁶ Thereby, these holes (positive carriers), representing a lack of negative carriers (electrons) in the valence band, are essential for the semiconductor sensitivity in gas sensing applications, mainly due to their ability to readily accept electrons. Thus, the interaction between borophene and gas molecules significantly varies depending on whether the gas acts as an electron donor or acceptor. J. Xu *et al.* obtained ultrathin borophene and subjected it to field-effect transistor (FET) measurements, unveiling its intrinsic p-type semiconductor behavior experimentally, coupled with a favorable carrier mobility of $1.26 \times 10^{-1} \text{ cm}^2 \text{ V}^{-1} \text{ s}^{-1}$.⁸⁴ Theoretical studies have predicted that an electric field can induce a tunable bandgap in β_{12} -borophene, leading to a transition from metallic to p-type semiconducting behavior, also influenced by charged impurities.¹⁵⁷

Electron-acceptor gases interact with borophene by withdrawing electrons from the 2D nanomaterial. This electron withdrawal leads to a greater concentration of holes, thereby enhancing the p-type conductivity of borophene through the heightened availability of these positive carriers. For instance, the adsorption of NO_2 onto borophene not only withdraws electrons but also reduces the Schottky barrier, resulting in a shift of the Fermi level closer to the valence band. This shift signifies the presence of the gas by causing a detectable increase in conductivity.¹⁵⁵ Conversely, the adsorption of electron-donor gases introduces additional electrons to borophene. These incoming electrons recombine with holes, reducing their density and consequently reducing the borophene conductivity due to the decreased availability of holes for current conduction.

Given the limited number of experimental studies focused on gas sensing with borophene to date, it is noteworthy to highlight a study where borophene, obtained through sonochemical exfoliation and decorated with barium, was employed for NO_2 detection.¹⁵⁸ The primary aim of using Ba was to lower the work function to enhance the sensing performance. Indeed, the response at room temperature (RT) to 25 ppm of NO_2 was substantially improved, from 24.1% to 51.5%, when comparing pristine and barium-decorated borophene. Similarly, the sensor sensitivity, given by the slopes of calibration curves, was improved from 0.848 to 0.984 %/ppm when borophene was decorated with barium. This enhanced performance when detecting NO_2 at ppm levels was observed in both, response (40s vs. 52s) and recovery times (52s vs. 59s), for barium-decorated versus pristine borophene, respectively. Furthermore, given that threshold limit values are often set at ppb levels, these results suggest the potential for achieving even faster response times.

However, as it is well-known in resistive gas sensors, selectivity is often limited as the active nanomaterials can interact with various gas compounds. To address this challenge, another study uses a borophene gas sensor with a mixed matrix membrane (MMM) comprising polyetherimide (PEI) incorporated into a zeolitic imidazole framework (ZIF-8).¹⁵⁵ This approach aimed for the PEI-ZIF-8 overlayer to serve as a selective membrane for NO_2 (Figure 6a) over other gaseous compounds like alcohols and hydrocarbons (Figure 6b). This study also investigated various ZIF-8 ratios (1:1, 1:2, 1:3, and 1:4 wt.%), finding that higher PEI content improved NO_2 selectivity. As the PEI

ratio increased, the overlayer was more efficient to selectively filter NO₂ without considerably reducing the sensing response. Specifically, a 1:4 ratio only reduced the response to NO₂ by 0.6% when detecting 25 ppm at room temperature and 35% relative humidity (RH). This configuration significantly improved NO₂ selectivity, reducing the response to other gases, such as CO₂, from 6.4% to 1.2% in the presence of the membrane. Additionally, the overlayer showed resistance to halogenated solvents, alcohols, and hydrocarbons. Indeed, as Figure 6c depicts, the responses to NO₂ were not compromised by the filtering overlayer. This MMM operates effectively under RT conditions, and notably, due to the hydrophobic nature of ZIF-8 and the humidity resistance of PEI, ambient moisture interference is mitigated. Additionally, it is essential to note that while the borophene sensor without the membrane experienced slight degradation after 35 days of use, the overlayer tended to protect the borophene-sensitive layer, thus mitigating degradation and increasing device lifetime, demonstrating notable repeatability (Figure 6d).¹⁵⁵ However, considering that NO₂ typically shows much higher sensing responses than gases such as volatile organic compounds (VOCs) due to larger charge transfers, a promising research avenue may involve the development of selective sensors tailored towards such gases.

Table 4 provides a comprehensive overview of the studies that have employed borophene gas sensors to date. It is worth noting that only a few of these studies have experimentally developed operative gas sensing devices. One significant parameter to consider is the method of synthesis. Most experimental borophene sensors have been produced through sonochemical methods, with a lesser number realized through CVD-based methods. This suggests that advanced techniques for producing borophene, such as MBE, still face significant challenges in terms of transferring the borophene and integrating it into electronic devices. The process of transferring borophene from the growth substrate to the target substrate without damaging its unique properties remains a challenge. Besides detecting NO₂, boron sheets produced via sonochemical exfoliation have been used to detect methane (CH₄) at RT, revealing suitable sensing performance in the ppm range.¹⁵⁹ This chemiresistive sensor achieved responses ranging from 43.5% to 153.1% for concentrations of 50 to 105 ppm, respectively. However, repeatability may be compromised by notable noise in resistance measurements. This study did not report on long-term stability or the impact of ambient humidity on sensor performance. Furthermore, significant hysteresis was observed, referring to a phenomenon where responses to specific gas concentrations vary depending on whether concentrations are being increased or decreased. Consequently, further investigation to reliably detect non-polar gases such as methane using borophene sensors is required.

C. Hou *et al.* reported a chemiresistive borophene sensor capable of detecting a wide range of NO₂ concentrations, achieving a remarkable 422% response for 100 ppm at RT conditions.¹⁶⁰ This borophene-based gas sensor shows promising response and recovery times (30s and 200s, respectively), aligning well with typical requirements for ambient monitoring applications. Furthermore, it demonstrates stability even after 1000 bending cycles, suggesting high possibilities for use in flexible electronics. However, it is worth noting that the experiments were conducted under an inert atmosphere (N₂). Therefore, for practical applications, the potential coexistence of oxygen in the same matrix should be thoroughly investigated. Nevertheless, the authors also explored the effect of ambient

moisture (RH levels between 0 and 60%) during NO₂ detection. Their findings experimentally reveal that water molecules exhibit an additive effect, increasing the response to NO₂.¹⁶⁰ These experimental findings align with theoretical predictions, which also indicate that NO₂ adsorption on borophene is energetically favorable and becomes even more stable in humid conditions.¹⁴⁸

Several trends can be deduced from Table 4 when comparing the sensing performances of borophene-based gas sensors. All sensors demonstrate the capability to operate effectively at RT, like graphene and other 2D nanomaterials. This presents inherent advantages such as lower power consumption, more straightforward and cost-effective device circuitry due to the absence of heating elements, and potentially extended device lifetime since borophene is not exposed to high temperatures. Another interesting parameter observed in experimental studies is the excellent signal-to-noise ratio of borophene. With responses in the tens of percentage range for ppm levels of various gases, borophene exhibits a high potential for detecting even lower concentrations, possibly reaching ppb levels. This is crucial for meeting the requirements of commercial applications such as ambient monitoring. Thus, there are still considerable research opportunities for exploring the borophene structure to detect NO₂ at low ppb levels. Additionally, research remains very limited on using this 2D nanomaterial for detecting gases other than NO₂, being its sensing properties largely unexplored in experimental contexts. This gap offers an interesting research avenue for future studies. Lastly, it is essential to highlight that all the sensors demonstrated response and recovery times within a few tens of seconds. This is paramount as it indicates noteworthy sensing dynamics, enabling the detection of even lower concentrations at ppb levels.

These conductivity changes, corresponding to the adsorption of gases with differing electronic properties, offer a measurable means to detect and quantify target gas analytes. However, various experimental conditions significantly affect the sensitivity towards specific compounds, including RH. Water molecules, predominantly acting as electron acceptors at ambient temperatures, can significantly interfere with gas sensing devices. Experimental findings suggest that the detection of electron-accepting gases like NO₂ is amplified at higher humidity levels due to an additive effect that increases the concentration of holes.¹⁶³ This effect contrasts with detecting electron-donating species in humid conditions, where a competitive reaction between water molecules and the analyte may reduce the sensor responses, contingent upon the relative humidity level.¹⁶⁴ Several experimental studies have observed that increased RH levels lead to higher sensing responses to NO₂ for borophene-based sensors, as water molecules and NO₂ act as electron acceptors.¹⁵⁸

In this perspective, C. Hou *et al.* developed a humidity sensor based on a heterostructure comprising borophene and graphene, with a mass ratio of 100:1.¹⁶¹ This study investigated the sensing performance for detecting H₂O from dry conditions to an 85% RH, revealing a remarkable increase in response of 4200% between both situations. Notably, the borophene-graphene heterostructure exhibited sensitivity to humidity nearly 700 times higher than that of pristine graphene, both in high-humidity environments and under bending strain. Similarly, a borophene-MoS₂ hybrid, with a mass ratio of 2:1, has been developed as a humidity sensor, further enhancing the sensing performance. This hybrid achieved a response of 15500% for an RH of 97%. Notably, the hybrid containing borophene

exhibited an approximately 80-fold increase in response compared to bare MoS₂.¹⁶² The authors attribute this enhanced humidity detection to several factors, like the large specific surface area, the presence of edge and defect sites such as S-vacancies, and the Grotthuss mechanism. Furthermore, this sensor showed reversible and sub-minute response and recovery times, highlighting its potential for practical uses in the future.

However, ambient moisture introduces further complications when detecting air pollutants, as the fluctuating relative humidity levels can impact the analyte detection accuracy. These variations necessitate comprehensive calibration processes to account for the influence of water molecules on sensor responses. For practical applications, it is essential to quantify the modulation in sensing performance induced by moisture to discount its effects and ensure reliable detection of target gases.

Another challenge lies in the relatively low resistance changes observed in borophene-based gas sensors compared to other nanomaterials, such as metal oxides (MOx). Specifically, the responses per unit concentration (e.g., ppm of NO₂) are significantly limited. It is important to recognize that the experimental results summarized in Table 4 were obtained at room temperature, which inherently leads to lower sensitivities compared to MOx sensors, typically operated at some hundreds of Celsius degrees. Nevertheless, further research efforts are likely required to enhance the overall response of borophene-based gas sensors.

Challenges and Limitations

Theoretical studies, derived under idealized conditions, help identify the most promising borophene configurations by predicting electronic properties, interactions with gases and the most stable phases. Despite the widespread recognition of borophene's high potential for use in the next generation of high-performance sensors, its practical application remains a significant challenge. A notable gap exists between theoretical and experimental research on borophene for sensing applications, characterized by a disproportionate ratio of theoretical works to experimental studies. This imbalance may come from several experimental factors, including challenges related to borophene oxidation, interference from relative humidity, and issues with selectivity, as will be discussed later. While these calculations provide crucial starting points for experimental exploration, their predictions should account for the practical challenges, to better support the development and optimization of borophene-based gas sensors.

From this perspective, there is still a lack of practical implementation of borophene gas sensors in commercial devices. Since this 2D nanomaterial is still in its early research stage, most studies have been conducted experimentally under controlled laboratory conditions. Therefore, advancing towards real-world applications requires addressing the experimental challenges identified in this section.

Superficial borophene oxidation. The susceptibility of borophene to oxidation, attributed to its high surface activity, represents a critical factor often overlooked in theoretical analyses. This tendency for oxidation can substantially modify the properties of borophene, presenting challenges for applying theoretical predictions in practical scenarios. While theoretical research extensively explores the properties of pure borophene, the practical challenge lies in obtaining and stabilizing borophene in real-world conditions where exposure to atmospheric oxygen is

unavoidable. This disparity highlights a significant gap between theoretical and experimental research on borophene for sensing applications, with most theoretical sensing studies not accounting for the borophene reactivity with oxygen.^{165,166}

One primary reason for this disparity might be the focus of theoretical studies on pristine borophene in ideal conditions, whereas, in practical scenarios, borophene exhibits considerable instability when exposed to atmospheric oxygen. Consequently, many experimental investigations report oxygen content ranging from 9% to 57% (Table 5), as evidenced by reliable techniques such as X-ray photoelectron spectroscopy (XPS). This oxygen incorporation can significantly alter the properties of borophene, potentially challenging the applicability of many theoretical studies. Moreover, theoretical studies often do not consider other elements, such as carbon and nitrogen, whereas experimental works frequently detect significant contents of these elements (Table 5). This surface contamination is primarily attributed to the borophene exposure to the air atmosphere and using solvents during the synthesis process. However, it is worth noting that specific methods, such as sonochemical exfoliation, can increase this surface contamination during the top-down method synthesis.

The presence of oxygen and carbon in borophene can also be attributed to defects in the borophene. These defects often act as reactive sites for interacting with gas molecules, significantly modifying the sensing performance. It is important to recognize these factors for accurate theoretical modeling and better alignment with experimental results.

Notably, experimental works frequently report high oxygen content in boron samples, necessitating careful consideration of boron suboxide (B_xO_y) and boron oxide (B_2O_3) presence, which appears at higher energy bindings in the B 1s peak. This phenomenon is illustrated in Figure 7. Research dating back to 1989 by Moddeman and collaborators studied boron oxidation in detail using pure boron powders.¹⁶⁷ This figure shows a comparison of boron 1s XPS peak at different take-off angles (α), ranging from 38° to 90° . A take-off angle of 90° indicates measurement from the horizontal sample surface, with photoelectrons being detected from deeper layers. At this angle, the main peak corresponds to B^0 (B-B bonds), while a secondary peak related to B_xO_y (B-O bonds) related to a suboxide layer can also be observed. However, as the take-off angle decreases, measuring progressively shallower depths, the intensity of suboxide layers (B_xO_y , where $x/y = 3$) tends to increase, suggesting that oxidation is concentrated near the surface. Additionally, a new and secondary peak at higher energy binding related to boron suboxide (B_xO_y , where $1.5 < x/y < 3$) emerges at lower angles, emphasizing the presence of a thin suboxide layer atop the boron surface. Beyond suboxide formation, fully oxidized boron (B_2O_3) may also form in the outermost layers of borophene.¹⁷¹ This fully oxidized state is identifiable in XPS spectra as a peak at higher binding energy in the B 1s, around 192.4 eV.¹⁷²

These experimental demonstrations are crucial for understanding the high levels of oxygen detected by XPS in recent publications on borophene-based works, as outlined in **Table 5**. This experimental evidence highlights the importance of accounting for surface oxidation in boron studies and should be factored into theoretical models. Further research into borophene oxidation mechanisms could reveal these surface changes, which are likely to

significantly affect the sensing performance. For instance, an impactful future study could involve performing XPS measurements at various take-off angles on few-layer borophene to more accurately quantify the ratios of B, O, and even C. Understanding the oxidation process more thoroughly upon air exposure could help in designing strategies to mitigate oxidation-related degradation, thus enhancing the borophene stability and functionality for gas sensing purposes.

Recently, X. Liu *et al.* studied the borophene oxidation process through two pathways. First, the exposure of borophene to air results in rapid oxidation within just 1 minute. Conversely, the oxidation process can be controlled if borophene is exposed to molecular oxygen in an ultra-high vacuum (UHV).⁷³ Despite shedding light on the superficial oxidation process of borophene, this methodology highlights a remaining challenge for applying borophene in ambient conditions due to uncontrolled oxidation processes.

R.Y. Guo *et al.* shed light on the oxidation mechanisms involving reactive dangling oxygen atoms. According to these authors, oxygen chemisorption on the borophene surface is an exergonic reaction that produces neutral and electrically active defects.¹⁶⁶ Initially, exposure of borophene to air generates dangling oxygen defects at the borophene surface, which are electrically neutral. However, upon the chemisorption of oxygen atoms, the borophene surface becomes polarized due to the difference in electronegativity between boron and oxygen. This polarization makes the surface more hydrophilic, possibly explaining the high sensitivity of borophene to ambient moisture. Specifically, partial electrons from borophene are likely transferred to adsorptive oxygen, partially filling the 2p orbitals. Moreover, unpaired electrons from oxygen can interact with a second oxygen atom to form more stable structures. This process results in the well-known surface oxidation of borophene, which is relatively stable due to chemisorbed oxygen with higher energy binding of more than 3 eV, as shown in Figure 8 for multiple configurations. Consequently, oxygen chemisorption is influenced by defects and impurities in borophene.¹⁶⁶

Furthermore, while it is feasible to maintain borophene under controlled laboratory conditions (e.g., dry boxes, nitrogen atmospheres), these environments diverge significantly from those encountered in real-world settings. While effective in preserving the integrity and stability of borophene for research purposes, such specialized conditions

may not be practical or economically viable for widespread sensor deployment and use. In this context, P. Ranjan *et al.* proposed an interesting approach to significantly reduce the undesired oxygen and carbon content, which involves performing an argon plasma surface etching.⁹⁸ However, since this strategy may only provide temporary effectiveness, there is yet to be a definitive solution for the rapid superficial oxidation of borophene. Hence, after this approach, borophene likely returns to some extent to the previous situation when exposed to air, in which oxygen remains a significant issue.

A novel strategy to enhance the stability of borophene is hydrogenation, leading to the formation of borophane, a hydrogenated derivative of borophene. Theoretical works suggest that borophane retains the exceptional properties of borophene, such as high Fermi velocity and Young's modulus while achieving dynamic stability through

electron transfer induced by hydrogenation.¹⁰⁹ Recent experimental efforts in 2023 by X. Zeng *et al.* have made significant advances toward synthesizing hydrogenated borophene (borophane) through exfoliation and ion exchange techniques. The resulting material, supported on a carbon substrate and decorated with platinum nanoparticles (Figure 9a), shows improved stability, although oxidation remains a concern. XPS survey spectra from this study revealed the presence of B, C, and Pt, as expected, but also a notable O 1s peak indicative of oxidation (Figure 9b). Further analysis of the B 1s peak deconvolution reveals a considerable amount of boron-oxygen (B-O) bonds (Figure 9d), pointing to oxidized boron.¹⁷³ Similarly, Q. Li *et al.* worked on synthesizing borophane polymorphs through hydrogenation, revealing a reduction in boron oxidation, although with detectable levels of boron oxide in XPS peaks.¹⁷⁴ Alternatively, Liu and collaborators reported the use bis(triphenylphosphine)copper tetrahydroborate as a boron source for obtaining β_{12} borophane through a CVD growth in a hydrogen-rich atmosphere.¹⁷⁵ This study reports a 6% of oxidation after 1h, which is a significant improvement in comparison to borophene (non-hydrogenated), but for implementing it in sensing devices is not enough. These findings highlight the persistent challenge of fully mitigating boron oxidation in hydrogenated borophene. While theoretical predictions and experimental advancements have showcased the potential of hydrogenation as a viable strategy for stabilizing borophene,^{176,177} further research is crucial to minimize the presence of boron oxide and fully realize the nanomaterial capabilities in sensing applications.

Recently, Rezvani and collaborators proposed a novel approach to face the oxidation issue, by using aluminum (Al)-activated chemical vapor deposition (CVD) to stabilize borophene.¹⁷⁸ Their findings reveal that Al aggregation on borophene reduces oxidation primarily to Al-rich areas and sheet edges, preserving the borophene γ_3 phase (with minor β_{12} phase) even after prolonged air exposure. DFT calculations confirmed that oxygen binding energy is significantly lower on Al-supported borophene than on metal-free borophene, aligning with the experimental observation of improved oxidation resistance. This Al-activation technique seems to limit the oxidation to the borophene edges, but it is an excellent starting point for developing further research to overcome this issue.

Interference of relative humidity. The impact of humidity on sensing performance is a critical consideration, as water molecules often represent the most prevalent interferent in sensor devices. As discussed previously, water molecules tend to act as electron acceptors, potentially interfering with the sensing process. In other words, the detection of air pollutants is highly dependent on the RH levels. Despite this, theoretical analyses frequently overlook this paramount effect, highlighting a significant discrepancy between theoretical predictions and experimental realities in the context of borophene-based sensors. Hence, a future avenue of research might involve DFT studies considering the sensing performance in a matrix where gas analytes coexist with ambient moisture.

Furthermore, the effect of water molecules is especially critical for borophene since its oxidation under exposure to air makes its surface highly hydrophilic. Besides, the exceptionally high sensing responses to ambient moisture summarized in Table 4 indicate that while borophene could act as a humidity sensor, detecting air pollutants in variable humidity levels constitutes a significant challenge. Considering the minimal amount of experimental work

employing borophene-based gas sensors, there is considerable room for novel developments. For instance, some anti-humidity strategies for resistive sensors are available.¹⁷⁹ A new research avenue for borophene-based devices could be using membranes to perform physical isolation. Membranes of different compositions, such as polylactic acid (PLA)¹⁸⁰ and polydimethylsiloxane (PDMS)^{181,182} have been employed for other nanomaterials to mitigate the interference of water molecules. However, as a trade-off, employing membranes to filter the ambient moisture to some extent increases the device complexity, cost, and maintenance.

Another issue with relative humidity is the potential instability of the active films. The sensing performance of Ba-decorated borophene was assessed over 35 days of use, revealing that 21% of RH does not compromise the stability, while 50% of RH dramatically decreases the sensor responses.¹⁵⁸ Thereby, a novel possibility for reducing the moisture interference and extending the borophene stability can be the development of heterostructures by adding nanomaterials with hydrophobic properties. In this sense, graphene can be an excellent choice thanks to its surface hydrophobicity and ability to work at RT as borophene. Indeed, this approach has already been employed in perovskites, which are well-known for fast degradation in contact with RH, and by combining them with graphene it is possible their protection for gas sensing purposes.^{183,184} Thereby, the combination of borophene with graphene has a significant potential to develop novel gas sensors. For instance, Liu and collaborators intercalated boron amongst graphene using an Ag(111) substrate.¹⁸⁵ Interestingly, the obtained borophene-graphene (B-G) heterostructures were bonded through Van der Waals forces in multilayer nanomaterial, while bilayers are covalently bonded. This change significantly modifies the heterostructure properties. Not limited to this, Wang and co-authors performed theoretical predictions over Van der Waals bonded B-G heterostructure doped with several transition metals.¹⁸⁶ According to this study, the metal doping significantly improves the sensing performance over organic molecules in comparison to the bare B-G, potentially being highly sensitive to C₂H₂ and HCHO.

Selectivity. Regarding selectivity, it is worth mentioning that the borophene potential to detect a broad spectrum of gas compounds, even at high purity levels, introduces a significant challenge due to its inherent lack of specificity. Like other 2D nanomaterials such as graphene or MoS₂, borophene may exhibit poor selectivity and cannot distinguish between gases coexisting within the same environment. A sophisticated approach to enhance selectivity is the use of filtering membranes with varying pore sizes for gas separation. This method controls the access of gas molecules to the sensor surface, improving the sensor ability to detect specific gases while reducing interference from others. Additionally, filtering membranes can prevent the adsorption of unwanted chemicals that could degrade the sensor material, potentially extending the sensor operational lifespan. A recent study by N.K. Arkoti *et al.* explored using a borophene gas sensor for NO₂ detection, employing a selective membrane. As a result, the use of this membrane significantly improved selectivity towards NO₂, and the filtering membrane's efficacy was particularly notable at higher humidity levels, enhancing the borophene gas sensor selectivity and stability.¹⁵⁵

However, integrating selective filtering membranes into gas sensors introduces several drawbacks. The addition of membranes increases the complexity of device design and fabrication, leading to higher production costs. Membranes may also require frequent maintenance, such as cleaning or replacement, particularly in environments with

dust, moisture, or other particulates that could block the pores, diminishing their effectiveness. Developing and fabricating specialized membranes that meet precise selectivity and permeability criteria can be resource intensive. Furthermore, the primary consideration for gas separation and filtering is the molecular size capable of diffusing through the membrane pores. Given the huge amount of compounds in real atmospheres, molecules of similar size might pass through the pores and reach the sensor surface, potentially resulting in false positives for analyte concentrations. This necessitates extensive research to achieve adequate selectivity under real conditions. Additionally, while filtering membranes improve selectivity, they may also restrict the flow of target gas molecules to the sensor surface, potentially decreasing the sensor sensitivity. This trade-off requires careful consideration during the sensor design process.

The nanomaterials inability to discriminate between different gases in complex matrices limits their applicability in real-world scenarios where multiple gases are present simultaneously. Thereby, researchers have turned to sensor arrays coupled with advanced data analysis techniques to overcome this limitation and enhance selectivity. Integrating multiple sensors with different compositions into an array offers a promising solution to the selectivity problem.¹⁸⁷⁻¹⁸⁹ Each sensor in the array responds differently to different gases based on its specific chemical interactions, providing a unique response pattern or "fingerprint" for each gas. Analyzing the sensor array responses makes it possible to distinguish between different gases, even in complex mixtures.¹⁹⁰ Moreover, sensor arrays can be tailored to target specific gases of interest, further enhancing selectivity.

Developing borophene-based sensor arrays with different compositions would be possible. This opens huge possibilities since it is possible to decorate borophene with metal nanoparticles, combine borophene with other 2D nanomaterials such as MoS₂ or graphene, or integrate them into metal oxide nanostructures. Once a sensor array with various cross-sensitivities is achieved, multivariate data methods like principal component regression (PCR), a method for multicomponent analysis, can be used. Besides, pattern recognition through principal component analysis (PCA) can also be employed, paving the way for developing machine learning tools.^{191,192} Combining these analyses would make it possible to identify the presence of specific gases and quantify their concentrations accurately.

Synthesis scalability. Addressing the scalability of borophene synthesis poses a significant challenge that probably prevents its use in practical applications. Currently, the MBE, which involves the growth of borophene on metal substrates, represents the predominant method for producing this 2D nanomaterial. However, this technique encounters limitations when considering the transition to industrial-scale production, primarily due to the limitations associated with maintaining precise control over the synthesis process on a larger scale. Additionally, as discussed previously, the MBE should face another significant challenge related to the transfer step. Despite the high-quality borophene obtained through the MBE method, when the 2D nanomaterial is transferred from the metal substrate to the device substrate (e.g., electrodes of sensing devices), this results in a lowering of borophene crystallinity, and in consequence, their properties are heavily affected.

For borophene to be viably synthesized for widespread industrial applications, alternative methods warrant exploration. Exploring top-down approaches remains a critical avenue for research. Innovations in ultrasonication-assisted liquid-phase exfoliation from bulk boron would lead to new methodologies for controlling the size and thickness of exfoliated sheets, which could overcome the current limitations. This method makes easier the large-scale production of borophene from existing bulk materials as a source. Nonetheless, this approach has its drawbacks. Specifically, sonochemical exfoliation may result in less control over the dimensions and uniformity of the borophene sheets produced. The variability in sheet size and thickness could affect the consistency of the material properties, posing challenges for applications that require precise specifications. Besides, it must be considered if synthesizing monolayer, bilayer, or multilayered borophene since their properties and synthesis costs can significantly change. Nevertheless, advancements in this area are essential for unlocking the full potential of borophene in industrial applications, making the large-scale production of this promising material a tangible reality.

Conclusions and Outlook

The miniaturization of sensors, driven by the unique properties of 2D nanomaterials, provides exceptional sensing properties. Their highest surface-to-volume ratio offers a greater density of available reactive sites for interacting with the gas compounds, significantly improving the sensing performance. Furthermore, advancements in scalable synthesis methods will be essential in enabling the large-scale production of high-quality borophene for practical sensor applications. In this sense, it is worth highlighting that ultrasonication-assisted liquid-phase exfoliation is a straightforward, cost-effective, and potentially scalable synthesis method.

Borophene, with its remarkable polymorphism, exceptional conductivity, and unparalleled flexibility, holds the potential to revolutionize materials science. Its unique properties offer unprecedented promise for gas sensing applications. However, upon reviewing the current state of borophene research in gas sensor applications, it is evident that while theoretical studies have shown the potential of borophene, there are significant challenges in translating these findings into practical applications. This highlights the crucial need to bridge the gap between theoretical predictions and experimental findings to gain a comprehensive understanding of borophene behavior in gas sensing applications. Both theoretical and experimental efforts are needed to address practical challenges, aligning theoretical models more closely with real-world conditions while advancing experimental techniques. Achieving this alignment will require overcoming several technological bottlenecks.¹⁹³

A critical challenge for the widespread adoption of borophene in sensing technologies is its instability in atmospheric conditions. Regardless of the borophene synthesis method used, borophene faces an invariable situation, its uncontrollable surface oxidation when exposed to air. Experimental findings using have shown that borophene samples exhibit a high oxygen content (tens of %) due to rapid oxidation within a few minutes of exposure to air. Hence, this suboxide layer on the borophene surface completely changes the sensing dynamics and performance of the sensors, jeopardizing the theoretical predictions that do not account for this phenomenon. Several approaches, such as borophene hydrogenation, can somewhat mitigate this problem, but the oxygen content is still significant. Another suggested strategy involves Ar plasma etching, which effectively removes oxygen from the borophene

surface. However, once the sample is removed from the vacuum chamber and exposed to the air, the oxidation process is expected to resume. Therefore, future advancements should focus on integrating material synthesis with device fabrication processes and developing surface protection techniques to improve the borophene stability against oxidation.

Another unresolved issue is the interference of relative humidity. As it is well-known, water molecules are probably the highest interferent compound for gas sensors. However, the superficial oxidation of borophene makes the surface highly hydrophilic, significantly enhancing the sensitivity to ambient moisture. Interestingly, borophene can potentially be used as a humidity sensor. Conversely, detecting air pollutants is challenging under variable humidity levels, which heavily affect the sensing performance. To address this challenge and enhance the reliability and long-term stability of borophene-based sensors, approaches such as using anti-humidity membranes and protective coatings can be effectively employed.

Additionally, it should be noted that, to date, borophene-based gas sensors exhibit limited responses per unit of pollutant concentration. This presents new research opportunities for improving sensing performance through various approaches, such as optimizing gas flow rates, moderately increasing operating temperatures, refining device design, and incorporating ultraviolet (UV) light to stimulate more energetic and effective interactions with gases.

Theoretical investigations have shown that borophene polymorphs can detect a wide variety of gas compounds. However, this sensitivity presents challenges for real-world applications due to the presence of multiple analytes in complex matrices like atmospheric conditions. In other words, when multiple gaseous compounds coexist in the same matrix, the discrimination and quantification of individual compounds remain a challenge. In this perspective, the development of sensor arrays that combine and analyze data may provide a solution to this issue. While this proposed solution offers promising avenues, it is accompanied by increased production costs, data processing complexities, and heightened device maintenance demands. These considerations necessitate a careful approach during the design phase to balance performance enhancements against practical constraints. Alternatively, considering the high versatility of borophene for surface engineering and the development of advanced nanocomposites, a practical pathway to improve selectivity might be creating new boron-based nanomaterials to tailor selectivity to some extent.

In summary, addressing issues such as borophene oxidation, interference from relative humidity, lack of selectivity, and synthesis scalability is crucial to enable the widespread use of borophene-based gas sensors. Researchers should focus on developing novel strategies to mitigate these challenges and position borophene as a leading candidate for high-performance electronic devices in the next generation of sensing technology.

Acknowledgments

J. C.-C. is supported by the Marie Skłodowska-Curie Postdoctoral Fellowship (Horizon Europe Programme) under grant agreement No. 101066282 "GREBOS".

References

(1) Tsujita, W.; Yoshino, A.; Ishida, H.; Moriizumi, T. Gas Sensor Network for Air-Pollution Monitoring. *Sens Actuators B Chem* **2005**, *110* (2), 304–311.

- (2) Idrees, Z.; Zheng, L. Low Cost Air Pollution Monitoring Systems: A Review of Protocols and Enabling Technologies. *J Ind Inf Integr* **2020**, *17*, 100123.
- (3) Djedouboum, A. C.; Ari, A. A. A.; Gueroui, A. M.; Mohamadou, A.; Aliouat, Z. Big Data Collection in Large-Scale Wireless Sensor Networks. *Sensors* **2018**, *18* (12), 4474.
- (4) Su, M.; Li, S.; Dravid, V. P. Miniaturized Chemical Multiplexed Sensor Array. *J Am Chem Soc* **2003**, *125* (33), 9930–9931.
- (5) Dahlin, A. B. Size Matters: Problems and Advantages Associated with Highly Miniaturized Sensors. *Sensors* **2012**, *12* (3), 3018–3036.
- (6) Hong, S.; Wu, M.; Hong, Y.; Jeong, Y.; Jung, G.; Shin, W.; Park, J.; Kim, D.; Jang, D.; Lee, J. H. FET-Type Gas Sensors: A Review. *Sens Actuators B Chem* **2021**, *330*, 129240.
- (7) Landaluce, H.; Arjona, L.; Perallos, A.; Falcone, F.; Angulo, I.; Muralter, F. A Review of IoT Sensing Applications and Challenges Using RFID and Wireless Sensor Networks. *Sensors* **2020**, *20* (9), 2495.
- (8) Schneider, P.; Castell, N.; Vogt, M.; Dauge, F. R.; Lahoz, W. A.; Bartonova, A. Mapping Urban Air Quality in near Real-Time Using Observations from Low-Cost Sensors and Model Information. *Environ Int* **2017**, *106*, 234–247.
- (9) Baron, R.; Saffell, J. Amperometric Gas Sensors as a Low Cost Emerging Technology Platform for Air Quality Monitoring Applications: A Review. *ACS Sens* **2017**, *2* (11), 1553–1566.
- (10) Choi, J. H.; Lee, J.; Byeon, M.; Hong, T. E.; Park, H.; Lee, C. Y. Graphene-Based Gas Sensors with High Sensitivity and Minimal Sensor-to-sensor Variation. *ACS Appl Nano Mater* **2020**, *3* (3), 2257–2265.
- (11) Zhang, Z.; Yang, Y.; Penev, E. S.; Yakobson, B. I. Elasticity, Flexibility, and Ideal Strength of Borophenes. *Adv Funct Mater* **2017**, *27* (9), 1605059.
- (12) Zhai, H. J.; Zhao, Y. F.; Li, W. L.; Chen, Q.; Bai, H.; Hu, H. S.; Piazza, Z. A.; Tian, W. J.; Lu, H. G.; Wu, Y. B.; Mu, Y. W.; Wei, G. F.; Liu, Z. P.; Li, J.; Li, S. D.; Wang, L. S. Observation of an All-Boron Fullerene. *Nature Chemistry* **2014**, *6* (8), 727–731.
- (13) Zdoğan, C. Ö.; Mukhopadhyay, S.; Hayami, W.; Güvenc, Z. B.; Pandey, R.; Boustani, S. The Unusually Stable B100 Fullerene, Structural Transitions in Boron Nanostructures, and a Comparative Study of α - and γ -Boron and Sheets. *Journal of Physical Chemistry C* **2010**, *114* (10), 4362–4375.
- (14) Shabbir, A.; Azeem, M. On the Partition Dimension of Tri-Hexagonal α -Boron Nanotube. *IEEE Access* **2021**, *9*, 55644–55653.
- (15) Xu, Y.; Xuan, X.; Yang, T.; Zhang, Z.; Li, S. D.; Guo, W. Quasi-Freestanding Bilayer Borophene on Ag(111). *Nano Lett* **2022**, *22* (8), 3488–3494.
- (16) Chahal, S.; Ranjan, P.; Motlag, M.; Yamijala, S. S. R. K. C.; Late, D. J.; Sadki, E. H. S.; Cheng, G. J.; Kumar, P. Borophene via Micromechanical Exfoliation. *Advanced Materials* **2021**, *33* (34), 2102039.
- (17) Hao, J.; Tai, G.; Zhou, J.; Wang, R.; Hou, C.; Guo, W. Crystalline Semiconductor Boron Quantum Dots. *ACS Appl Mater Interfaces* **2020**, *12* (15), 17669–17675.
- (18) Paul Choudhury, S.; Feng, Z.; Gao, C.; Ma, X.; Zhan, J.; Jia, F. BN Quantum Dots Decorated ZnO Nanoplates Sensor for Enhanced Detection of BTEX Gases. *J Alloys Compd* **2020**, *815*, 152376.
- (19) Wang, H.; An, D.; Wang, M.; Sun, L.; Li, Y.; Li, N.; Hu, S.; He, Y. B. Crystalline Borophene Quantum Dots and Their Derivative Boron Nanospheres. *Mater Adv* **2021**, *2* (10), 3269–3273.
- (20) Wang, Z.; Zhu, L.; Sun, S.; Wang, J.; Yan, W. One-Dimensional Nanomaterials in Resistive Gas Sensor: From Material Design to Application. *Chemosensors* **2021**, *Vol. 9, Page 198* **2021**, *9* (8), 198.
- (21) Xu, T. T.; Zheng, J. G.; Wu, N.; Nicholls, A. W.; Roth, J. R.; Dikin, D. A.; Ruoff, R. S. Crystalline Boron Nanoribbons: Synthesis and Characterization. *Nano Lett* **2004**, *4* (5), 963–968.
- (22) Zhong, Q.; Kong, L.; Gou, J.; Li, W.; Sheng, S.; Yang, S.; Cheng, P.; Li, H.; Wu, K.; Chen, L. Synthesis of Borophene Nanoribbons on Ag(110) Surface. *Phys Rev Mater* **2017**, *1* (2), 021001.
- (23) Otten, C. J.; Lourie, O. R.; Yu, M. F.; Cowley, J. M.; Dyer, M. J.; Ruoff, R. S.; Buhro, W. E. Crystalline Boron Nanowires. *J Am Chem Soc* **2002**, *124* (17), 4564–4565.
- (24) Zhang, Y.; Ago, H.; Yumura, M.; Komatsu, T.; Ohshima, S.; Uchida, K.; Iijima, S. Synthesis of Crystalline Boron Nanowires by Laser Ablation. *Chemical Communications* **2002**, *2* (23), 2806–2807.
- (25) Meng, X. M.; Hu, J. Q.; Jiang, Y.; Lee, C. S.; Lee, S. T. Boron Nanowires Synthesized by Laser Ablation at High Temperature. *Chem Phys Lett* **2003**, *370* (5–6), 825–828.
- (26) Cao, L. M.; Zhang, Z.; Sun, L. L.; Gao, C. X.; He, M.; Wang, Y. Q.; Li, Y. C.; Zhang, X. Y.; Li, G.; Zhang, J.; Wang, W. K. Well-Aligned Boron Nanowire Arrays. *Advanced Materials* **2001**, *13* (22), 1701–1704.
- (27) Tian, J.; Cai, J.; Hui, C.; Zhang, C.; Bao, L.; Gao, M.; Shen, C.; Gao, H. Boron Nanowires for Flexible Electronics. *Appl Phys Lett* **2008**, *93* (12).
- (28) Patel, R. B.; Chou, T.; Iqbal, Z. Synthesis of Boron Nanowires, Nanotubes, and Nanosheets. *J Nanomater* **2015**, *2015* (1), 243925.
- (29) Li, J. L.; He, T.; Yang, G. Ferromagnetism and Semiconducting of Boron Nanowires. *Nanoscale Res Lett* **2012**, *7* (1), 1–6.
- (30) Yang, W.; Gan, L.; Li, H.; Zhai, T. Two-Dimensional Layered Nanomaterials for Gas-Sensing Applications. *Inorg Chem Front* **2016**, *3* (4), 433–451.
- (31) Zhang, L.; Khan, K.; Zou, J.; Zhang, H.; Li, Y. Recent Advances in Emerging 2D Material-Based Gas Sensors: Potential in Disease Diagnosis. *Adv Mater Interfaces* **2019**, *6* (22), 1901329.
- (32) Kiani, M.; Rehman, M. U.; Tian, X.; Yakobson, B. Two-Dimensional Nanomaterials for the Development of Efficient Gas Sensors: Recent Advances, Challenges, and Future Perspectives. *Adv Mater Technol* **2022**, *7* (7), 2101252.
- (33) Choi, S. J.; Kim, I. D. Recent Developments in 2D Nanomaterials for Chemiresistive-Type Gas Sensors. *Electronic Materials Letters* **2018**, *14* (3), 221–260.
- (34) Pawar, K. K.; Kumar, A.; Mirzaei, A.; Kumar, M.; Kim, H. W.; Kim, S. S. 2D Nanomaterials for Realization of Flexible and Wearable Gas Sensors: A Review. *Chemosphere* **2024**, *352*, 141234.
- (35) Hou, C.; Tai, G.; Liu, Y.; Liu, R.; Liang, X.; Wu, Z.; Wu, Z. Borophene Pressure Sensing for Electronic Skin and Human-Machine Interface. *Nano Energy* **2022**, *97*, 107189.
- (36) Geim, A. K. Graphene: Status and Prospects. *Science (1979)* **2009**, *324* (5934), 1530–1534.
- (37) Castro Neto, A. H.; Guinea, F.; Peres, N. M. R.; Novoselov, K. S.; Geim, A. K. The Electronic Properties of Graphene. *Rev Mod Phys* **2009**, *81* (1), 109–162.

- (38) Fathy, M.; Gomaa, A.; Taher, F. A.; El-Fass, M. M.; Kashyout, A. E. H. B. Optimizing the Preparation Parameters of GO and RGO for Large-Scale Production. *J Mater Sci* **2016**, *51* (12), 5664–5675.
- (39) Yin, X.; Tang, C. S.; Zheng, Y.; Gao, J.; Wu, J.; Zhang, H.; Chhowalla, M.; Chen, W.; Wee, A. T. S. Recent Developments in 2D Transition Metal Dichalcogenides: Phase Transition and Applications of the (Quasi-)Metallic Phases. *Chem Soc Rev* **2021**, *50* (18), 10087–10115.
- (40) Zhang, K.; Feng, Y.; Wang, F.; Yang, Z.; Wang, J. Two Dimensional Hexagonal Boron Nitride (2D-HBN): Synthesis, Properties and Applications. *J Mater Chem C Mater* **2017**, *5* (46), 11992–12022.
- (41) Kumar, R.; Sahoo, S.; Joanni, E.; Singh, R. K.; Yadav, R. M.; Verma, R. K.; Singh, D. P.; Tan, W. K.; Pérez del Pino, A.; Moshkalev, S. A.; Matsuda, A. A Review on Synthesis of Graphene, h-BN and MoS₂ for Energy Storage Applications: Recent Progress and Perspectives. *Nano Res* **2019**, *12* (11), 2655–2694.
- (42) Hosseini, S. M.; Imanpour, A.; Rezavand, M.; Arjmandi Tash, A. M.; Antonini, S.; Rezvani, S. J.; Abdi, Y. Electrochemoresistance Sensor: A Borophene-Based Sensor with Simultaneous Electrochemical and Chemoresistance Sensing Capability. *ACS Mater Lett* **2024**, *6* (3), 933–942.
- (43) Kaimal, R.; Maridevaru, M. C.; Dube, A.; Wu, J. J.; Sambandam, A.; Ashokkumar, M. Borophene Nanosheet-Based Electrochemical Sensing toward Groundwater Arsenic Detection. *Ind Eng Chem Res* **2023**, *62* (38), 15418–15427.
- (44) Ranjan, P.; Lee, J. M.; Kumar, P.; Vinu, A. Borophene: New Sensation in Flatland. *Advanced Materials* **2020**, *32* (34), 2000531.
- (45) Boustani, I. Systematic Ab Initio Investigation of Bare Boron Clusters: MDetermination of the Geometry and Electronic Structures of B_n (n=2–14). *Phys Rev B* **1997**, *55* (24), 16426.
- (46) Erakulan, E. S.; Thapa, R. Origin of Pure and C Doped Borophene Stability and Its Activity for OER. *Appl Surf Sci* **2022**, *574*, 151613.
- (47) Tang, H.; Ismail-Beigi, S. Novel Precursors for Boron Nanotubes: The Competition of Two-Center and Three-Center Bonding in Boron Sheets. *Phys Rev Lett* **2007**, *99* (11), 115501.
- (48) Mannix, A. J.; Zhou, X. F.; Kiraly, B.; Wood, J. D.; Alducin, D.; Myers, B. D.; Liu, X.; Fisher, B. L.; Santiago, U.; Guest, J. R.; Yacaman, M. J.; Ponce, A.; Oganov, A. R.; Hersam, M. C.; Guisinger, N. P. Synthesis of Borophenes: Anisotropic, Two-Dimensional Boron Polymorphs. *Science* (1979) **2015**, *350* (6267), 1513–1516.
- (49) Piazza, Z. A.; Hu, H. S.; Li, W. L.; Zhao, Y. F.; Li, J.; Wang, L. S. Planar Hexagonal B36 as a Potential Basis for Extended Single-Atom Layer Boron Sheets. *Nat Commun* **2014**, *5* (1), 1–6.
- (50) Feng, B.; Sugino, O.; Liu, R. Y.; Zhang, J.; Yukawa, R.; Kawamura, M.; Iimori, T.; Kim, H.; Hasegawa, Y.; Li, H.; Chen, L.; Wu, K.; Kumigashira, H.; Komori, F.; Chiang, T. C.; Meng, S.; Matsuda, I. Dirac Fermions in Borophene. *Phys Rev Lett* **2017**, *118* (9), 096401.
- (51) Jiao, Y.; Ma, F.; Bell, J.; Bilic, A.; Du, A. Two-Dimensional Boron Hydride Sheets: High Stability, Massless Dirac Fermions, and Excellent Mechanical Properties. *Angewandte Chemie International Edition* **2016**, *55* (35), 10292–10295.
- (52) Gupta, G. H.; Kadakia, S.; Agiwal, D.; Keshari, T.; Kumar, S. Borophene Nanomaterials: Synthesis and Applications in Biosensors. *Mater Adv* **2024**, *5* (5), 1803–1816.
- (53) Shukla, V.; Wärnå, J.; Jena, N. K.; Grigoriev, A.; Ahuja, R. Toward the Realization of 2D Borophene Based Gas Sensor. *Journal of Physical Chemistry C* **2017**, *121* (48), 26869–26876.
- (54) Li, W.; Kong, L.; Chen, C.; Gou, J.; Sheng, S.; Zhang, W.; Li, H.; Chen, L.; Cheng, P.; Wu, K. Experimental Realization of Honeycomb Borophene. *Sci Bull (Beijing)* **2018**, *63* (5), 282–286.
- (55) Feng, B.; Zhang, J.; Zhong, Q.; Li, W.; Li, S.; Li, H.; Cheng, P.; Meng, S.; Chen, L.; Wu, K. Experimental Realization of Two-Dimensional Boron Sheets. *Nat Chem* **2016**, *8* (6), 563–568.
- (56) Mortazavi, B.; Makaremi, M.; Shahrokhi, M.; Raeisi, M.; Singh, C. V.; Rabczuk, T.; Pereira, L. F. C. Borophene Hydride: A Stiff 2D Material with High Thermal Conductivity and Attractive Optical and Electronic Properties. *Nanoscale* **2018**, *10* (8), 3759–3768.
- (57) Tai, G.; Liu, B.; Hou, C.; Shao, W.; Wu, Z.; Wang, X.; Wu, R.; Xu, T.; Gao, Y. Mechanical and Electrical Properties of Borophene and Its Band Structure Modulation via Strain and Electric Fields: A First-Principles Study. *Mater Res Express* **2021**, *8* (6), 065003.
- (58) Wang, Z. Q.; Lü, T. Y.; Wang, H. Q.; Feng, Y. P.; Zheng, J. C. Review of Borophene and Its Potential Applications. *Front Phys (Beijing)* **2019**, *14* (3), 1–20.
- (59) Rahman, A.; Rahman, M. T.; Chowdhury, M. A.; Bin Ekram, S.; Uddin, M. M. K.; Islam, M. R.; Dong, L. Emerging 2D Borophene: Synthesis, Characterization, and Sensing Applications. *Sens Actuators A Phys* **2023**, *359*, 114468.
- (60) Chand, H.; Kumar, A.; Krishnan, V. Borophene and Boron-Based Nanosheets: Recent Advances in Synthesis Strategies and Applications in the Field of Environment and Energy. *Adv Mater Interfaces* **2021**, *8* (15), 2100045.
- (61) Richards, R. D.; Bailey, N. J.; Liu, Y.; Rockett, T. B. O.; Mohmad, A. R. GaAsBi: From Molecular Beam Epitaxy Growth to Devices. *physica status solidi (b)* **2022**, *259* (2), 2100330.
- (62) Nunn, W.; Truttman, T. K.; Jalan, B. A Review of Molecular-Beam Epitaxy of Wide Bandgap Complex Oxide Semiconductors. *J Mater Res* **2021**, *36* (23), 4846–4864.
- (63) Penev, E. S.; Kutana, A.; Yakobson, B. I. Can Two-Dimensional Boron Superconduct? *Nano Lett* **2016**, *16* (4), 2522–2526.
- (64) Zhang, Z.; Yang, Y.; Gao, G.; Yakobson, B. I. Two-Dimensional Boron Monolayers Mediated by Metal Substrates. *Angewandte Chemie* **2015**, *127* (44), 13214–13218.
- (65) Xu, S.; Zhao, Y.; Liao, J.; Yang, X.; Xu, H. The Nucleation and Growth of Borophene on the Ag (111) Surface. *Nano Res* **2016**, *9* (9), 2616–2622.
- (66) Liu, X.; Zhang, Z.; Wang, L.; Yakobson, B. I.; Hersam, M. C. Intermixing and Periodic Self-Assembly of Borophene Line Defects. *Nat Mater* **2018**, *17* (9), 783–788.
- (67) Zhang, Z.; Mannix, A. J.; Hu, Z.; Kiraly, B.; Guisinger, N. P.; Hersam, M. C.; Yakobson, B. I. Substrate-Induced Nanoscale Undulations of Borophene on Silver. *Nano Lett* **2016**, *16* (10), 6622–6627.
- (68) Tai, G.; Hu, T.; Zhou, Y.; Wang, X.; Kong, J.; Zeng, T.; You, Y.; Wang, Q. Synthesis of Atomically Thin Boron Films on Copper Foils. *Angewandte Chemie International Edition* **2015**, *54* (51), 15473–15477.
- (69) Kiraly, B.; Liu, X.; Wang, L.; Zhang, Z.; Mannix, A. J.; Fisher, B. L.; Yakobson, B. I.; Hersam, M. C.; Guisinger, N. P. Borophene Synthesis on Au(111). *ACS Nano* **2019**, *13* (4), 3816–3822.
- (70) Vinogradov, N. A.; Lyalin, A.; Taketsugu, T.; Vinogradov, A. S.; Preobrajenski, A. Single-Phase Borophene on Ir(111): Formation, Structure, and Decoupling from the Support. *ACS Nano* **2019**, *13* (12), 14511–14518.
- (71) Peng, B.; Zhang, H.; Shao, H.; Xu, Y.; Zhang, R.; Zhu, H. The Electronic, Optical, and Thermodynamic Properties of Borophene from First-Principles Calculations. *J Mater Chem C Mater* **2016**, *4* (16), 3592–3598.

- (72) Zhang, Z.; Penev, E. S.; Jakobson, B. I. Polyphony in B Flat. *Nat Chem* **2016**, *8* (6), 525–527.
- (73) Liu, X.; Rahn, M. S.; Ruan, Q.; Jakobson, B. I.; Hersam, M. C. Probing Borophene Oxidation at the Atomic Scale. *Nanotechnology* **2022**, *33* (23), 235702.
- (74) Liu, X.; Li, Q.; Ruan, Q.; Rahn, M. S.; Jakobson, B. I.; Hersam, M. C. Borophene Synthesis beyond the Single-Atomic-Layer Limit. *Nat Mater* **2021**, *21* (1), 35–40.
- (75) Chen, C.; Lv, H.; Zhang, P.; Zhuo, Z.; Wang, Y.; Ma, C.; Li, W.; Wang, X.; Feng, B.; Cheng, P.; Wu, X.; Wu, K.; Chen, L. Synthesis of Bilayer Borophene. *Nat Chem* **2021**, *14* (1), 25–31.
- (76) Li, H.; Yang, J.; Ma, Y.; Liu, G.; Xu, X.; Huo, Z.; Chen, J.; Li, J.; Zhang, W.; Wang, K.; Chen, L.; Xiao, X. Monolayer Borophene Formation on Cu(111) Surface Triggered by $\langle 11\bar{0} \rangle$ Step Edge. *Small* **2024**, *20* (7), 2303502.
- (77) Heindel, J. P.; Xantheas, S. S. Molecular Dynamics Driven by the Many-Body Expansion (MBE-MD). *J Chem Theory Comput* **2021**, *17* (12), 7341–7352.
- (78) Yan, P.; Lin, R.; Ruan, S.; Liu, A.; Chen, H.; Zheng, Y.; Chen, S.; Guo, C.; Hu, J. A Practical Topological Insulator Saturable Absorber for Mode-Locked Fiber Laser. *Sci Rep* **2015**, *5* (1), 1–5.
- (79) Wu, R.; Drozdov, I. K.; Eltinge, S.; Zahl, P.; Ismail-Beigi, S.; Božović, I.; Gozar, A. Large-Area Single-Crystal Sheets of Borophene on Cu(111) Surfaces. *Nat Nanotechnol* **2018**, *14* (1), 44–49.
- (80) Tang, L.; Tan, J.; Nong, H.; Liu, B.; Cheng, H. M. Chemical Vapor Deposition Growth of Two-Dimensional Compound Materials: Controllability, Material Quality, and Growth Mechanism. *Acc Mater Res* **2021**, *2* (1), 36–47.
- (81) Bhowmik, S.; Govind Rajan, A. Chemical Vapor Deposition of 2D Materials: A Review of Modeling, Simulation, and Machine Learning Studies. *iScience* **2022**, *25* (3), 103832.
- (82) Cuxart, M. G.; Seufert, K.; Chesnyak, V.; Waqas, W. A.; Robert, A.; Bocquet, M. L.; Duesberg, G. S.; Sachdev, H.; Auwärter, W. Borophenes Made Easy. *Sci Adv* **2021**, *7* (45), 1490.
- (83) Mazaheri, A.; Javadi, M.; Abdi, Y. Chemical Vapor Deposition of Two-Dimensional Boron Sheets by Thermal Decomposition of Diborane. *ACS Appl Mater Interfaces* **2021**, *13* (7), 8844–8850.
- (84) Xu, J.; Chang, Y.; Gan, L.; Ma, Y.; Zhai, T.; Xu, J. Q.; Chang, Y. Y.; Gan, L.; Ma, Y.; Zhai, T. Y. Ultrathin Single-Crystalline Boron Nanosheets for Enhanced Electro-Optical Performances. *Advanced Science* **2015**, *2* (6), 1500023.
- (85) Guo, Z.; Lin, H.; Zhang, H.; Tian, Y.; Chen, Y.; Chen, J.; Deng, S.; Liu, F. Low-Pressure CVD Synthesis of Tetragonal Borophene Single-Crystalline Sheets with High Ambient Stability. *Cryst Growth Des* **2023**, *23* (6), 4506–4513.
- (86) Tai, G.; Xu, M.; Hou, C.; Liu, R.; Liang, X.; Wu, Z. Borophene Nanosheets as High-Efficiency Catalysts for the Hydrogen Evolution Reaction. *ACS Appl Mater Interfaces* **2021**, *13* (51), 60987–60994.
- (87) Wu, Z.; Tai, G.; Liu, R.; Shao, W.; Hou, C.; Liang, X. Synthesis of Borophene on Quartz towards Hydroelectric Generators. *J Mater Chem A Mater* **2022**, *10* (15), 8218–8226.
- (88) Jomphoak, A.; Phokharatkul, D.; Eiamchai, P. Non-Toxic Precursor for Chemical Vapor Deposition of Borophene on Cu(111) Surface. *Mater Chem Phys* **2023**, *299*, 127527.
- (89) Sun, D.; Song, X.; Liu, L.; Song, C.; Liu, H.; Li, Q.; Butler, K.; Xie, C.; Zhang, Z.; Xie, Y. Ab Initio Kinetic Pathway of Diborane Decomposition on Transition Metal Surfaces in Borophene Chemical Vapor Deposition Growth. *Journal of Physical Chemistry Letters* **2024**, 9668–9676.
- (90) Li, H.; Jing, L.; Liu, W.; Lin, J.; Tay, R. Y.; Tsang, S. H.; Teo, E. H. T. Scalable Production of Few-Layer Boron Sheets by Liquid-Phase Exfoliation and Their Superior Supercapacitive Performance. *ACS Nano* **2018**, *12* (2), 1262–1272.
- (91) Adekoya, G. J.; Adekoya, O. C.; Muloiwa, M.; Sadiku, E. R.; Kupolati, W. K.; Hamam, Y. Advances In Borophene: Synthesis, Tunable Properties, and Energy Storage Applications. *Small* **2024**, *20* (40), 2403656.
- (92) Karikalani, N.; Elavarasan, M.; Yang, T. C. K. Effect of Cavitation Erosion in the Sonochemical Exfoliation of Activated Graphite for Electrocatalysis of Acetololol. *Ultrason Sonochem* **2019**, *56*, 297–304.
- (93) Gosch, J.; Synnatschke, K.; Stock, N.; Backes, C. Comparative Study of Sonication-Assisted Liquid Phase Exfoliation of Six Layered Coordination Polymers. *Chemical Communications* **2022**, *59* (1), 55–58.
- (94) Gu, X.; Zhao, Y.; Sun, K.; Vieira, C. L. Z.; Jia, Z.; Cui, C.; Wang, Z.; Walsh, A.; Huang, S. Method of Ultrasound-Assisted Liquid-Phase Exfoliation to Prepare Graphene. *Ultrason Sonochem* **2019**, *58*, 104630.
- (95) Zhang, F.; She, L.; Jia, C.; He, X.; Li, Q.; Sun, J.; Lei, Z.; Liu, Z. H. Few-Layer and Large Flake Size Borophene: Preparation with Solvothermal-Assisted Liquid Phase Exfoliation. *RSC Adv* **2020**, *10* (46), 27532–27537.
- (96) Guo, L.; Wang, H.; Wu, Z.; Yang, X.; Ma, R.; Hu, Y.; Li, G.; Shi, D.; Xie, W.; Zhang, W.; Lan, F.; Zhou, L.; Zhang, K. Li-Intercalation Chemistry of Few-Layer Borophene with Ultrahigh Capacity and Fast Kinetics. *Chemical Engineering Journal* **2023**, *473*, 145017.
- (97) Radhakrishnan, S.; Padmanabhan, N. T.; Mathews, A. J.; Tang, Y.; Santhanakrishnan, T.; John, H. Surfactant-Assisted Restructuring of Boron to Borophene: Implications for Enhanced Hydrogen Evolution. *ACS Appl Nano Mater* **2024**, *7* (11), 12564–12578.
- (98) Ranjan, P.; Sahu, T. K.; Bhushan, R.; Yamijala, S. S. R. K. C.; Late, D. J.; Kumar, P.; Vinu, A. Freestanding Borophene and Its Hybrids. *Advanced Materials* **2019**, *31* (27), 1900353.
- (99) Rajput, U.; Akhtar, M. F.; Walve, V.; Mulani, I.; Vyas, G.; Bhowmick, S.; Kumar, P.; Deshpande, A. Liquid Phase Exfoliated Borophene on Au(111). *Journal of Physical Chemistry C* **2024**, *128* (9), 4104–4110.
- (100) Najiya, K. P. P.; Konnola, R.; Sreena, T. S.; Solomon, S.; Gopchandran, K. G. Liquid Phase Exfoliation of Few-Layer Borophene with High Hole Mobility for Low-Power Electronic Devices. *Inorg Chem Commun* **2024**, *168*, 112962.
- (101) Lin, H.; Shi, H.; Wang, Z.; Mu, Y.; Li, S.; Zhao, J.; Guo, J.; Yang, B.; Wu, Z. S.; Liu, F. Scalable Production of Freestanding Few-Layer B12-Borophene Single Crystalline Sheets as Efficient Electrocatalysts for Lithium-Sulfur Batteries. *ACS Nano* **2021**, *15* (11), 17327–17336.
- (102) Sahoo, B. B.; Pandey, V. S.; Dogonchi, A. S.; Thatoi, D. N.; Nayak, N.; Nayak, M. K. Exploring the Potential of Borophene-Based Materials for Improving Energy Storage in Supercapacitors. *Inorg Chem Commun* **2023**, *154*, 110919.
- (103) Zhang, X.; Hu, J.; Cheng, Y.; Yang, H. Y.; Yao, Y.; Yang, S. A. Borophene as an Extremely High Capacity Electrode Material for Li-Ion and Na-Ion Batteries. *Nanoscale* **2016**, *8* (33), 15340–15347.
- (104) Wu, Z.; Tai, G.; Liu, R.; Hou, C.; Shao, W.; Liang, X.; Wu, Z. Van Der Waals Epitaxial Growth of Borophene on a Mica Substrate toward a High-Performance Photodetector. *ACS Appl Mater Interfaces* **2021**, *13* (27), 31808–31815.
- (105) Hou, C.; Tai, G.; Liu, Y.; Wu, Z.; Liang, X.; Liu, X. Borophene-Based Materials for Energy, Sensors and Information Storage Applications. *Nano Research Energy* **2023**, *2* (2).

- (106) Yang, R.; Sun, M. Borophenes: Monolayer, Bilayer and Heterostructures. *J Mater Chem C Mater* **2023**, *11* (21), 6834–6846.
- (107) Feng, B.; Zhang, J.; Ito, S.; Arita, M.; Cheng, C.; Chen, L.; Wu, K.; Komori, F.; Sugino, O.; Miyamoto, K.; Okuda, T.; Meng, S.; Matsuda, I. Discovery of 2D Anisotropic Dirac Cones. *Advanced Materials* **2018**, *30* (2), 1704025.
- (108) Cheng, T.; Lang, H.; Li, Z.; Liu, Z.; Liu, Z. Anisotropic Carrier Mobility in Two-Dimensional Materials with Tilted Dirac Cones: Theory and Application. *Physical Chemistry Chemical Physics* **2017**, *19* (35), 23942–23950.
- (109) Xu, L. C.; Du, A.; Kou, L. Hydrogenated Borophene as a Stable Two-Dimensional Dirac Material with an Ultrahigh Fermi Velocity. *Physical Chemistry Chemical Physics* **2016**, *18* (39), 27284–27289.
- (110) Wang, Z.; Lü, T. Y.; Wang, H. Q.; Feng, Y. P.; Zheng, J. C. High Anisotropy of Fully Hydrogenated Borophene. *Physical Chemistry Chemical Physics* **2016**, *18* (46), 31424–31430.
- (111) Mortazavi, B.; Rahaman, O.; Dianat, A.; Rabczuk, T. Mechanical Responses of Borophene Sheets: A First-Principles Study. *Physical Chemistry Chemical Physics* **2016**, *18* (39), 27405–27413.
- (112) Peköz, R.; Konuk, M.; Kilic, M. E.; Durgun, E. Two-Dimensional Fluorinated Boron Sheets: Mechanical, Electronic, and Thermal Properties. *ACS Omega* **2018**, *3* (2), 1815–1822.
- (113) Hou, C.; Tai, G.; Hao, J.; Sheng, L.; Liu, B.; Wu, Z. Ultrastable Crystalline Semiconducting Hydrogenated Borophene. *Angewandte Chemie International Edition* **2020**, *59* (27), 10819–10825.
- (114) Shen, J.; Yang, Z.; Wang, Y.; Xu, L. C.; Liu, R.; Liu, X. The Gas Sensing Performance of Borophene/MoS₂ Heterostructure. *Appl Surf Sci* **2020**, *504*, 144412.
- (115) Arefi, V.; Horri, A.; Tavakoli, M. B. Transport Properties of Na-Decorated Borophene under CO/CO₂ Adsorption. *Comput Theor Chem* **2021**, *1197*, 113159.
- (116) Tu, X.; Xu, H.; Wang, X.; Li, C.; Fan, G.; Chu, X. First-Principles Study of Pristine and Li-Doped Borophene as a Candidate to Detect and Scavenge SO₂ Gas. *Nanotechnology* **2021**, *32* (32), 325502.
- (117) Li, W.; Jiang, Q.; Li, D.; Ao, Z.; An, T. Density Functional Theory Investigation on Selective Adsorption of VOCs on Borophene. *Chinese Chemical Letters* **2021**, *32* (9), 2803–2806.
- (118) Shen, J.; Yang, Z.; Wang, Y.; Xu, L. C.; Liu, R.; Liu, X. Organic Gas Sensing Performance of the Borophene van Der Waals Heterostructure. *Journal of Physical Chemistry C* **2021**, *125* (1), 427–435.
- (119) Omidvar, A. Borophene: A Novel Boron Sheet with a Hexagonal Vacancy Offering High Sensitivity for Hydrogen Cyanide Detection. *Comput Theor Chem* **2017**, *1115*, 179–184.
- (120) Sun, Q.; Yang, Z.; Huo, Y.; Liu, R.; Xu, L. C.; Xue, L.; Liu, X. Designing and Optimizing B₁-Borophene Organic Gas Sensor: A Theoretical Study. *Surf Sci* **2022**, *719*, 122030.
- (121) Wang, C. B.; Tian, Y. P.; Duan, J. X.; Zhang, B. Y.; Gong, W. J. Enhanced Organic Gas Sensing Performance of Borophene/Graphene van Der Waals Heterostructures via Transition Metal Doping. *Surfaces and Interfaces* **2023**, *43*, 103544.
- (122) Opoku, F.; Govender, P. P. Highly Selective and Sensitive Detection of Formaldehyde by B₁₂-Borophene/SnO₂ Heterostructures: The Role of an External Electric Field and In-Plane Biaxial Strain. *Journal of Physical Chemistry A* **2020**, *124* (11), 2288–2300.
- (123) Yu, H. S.; Li, S. L.; Truhlar, D. G. Perspective: Kohn-Sham Density Functional Theory Descending a Staircase. *Journal of Chemical Physics* **2016**, *145* (13), 130901.
- (124) Grimme, S.; Waletzke, M. A Combination of Kohn-Sham Density Functional Theory and Multi-Reference Configuration Interaction Methods. *J Chem Phys* **1999**, *111* (13), 5645–5655.
- (125) Li, Z.; Smeu, M.; Afsari, S.; Xing, Y.; Ratner, M. A.; Borguet, E. Single-Molecule Sensing of Environmental PH—an STM Break Junction and NEGF-DFT Approach. *Angewandte Chemie International Edition* **2014**, *53* (4), 1098–1102.
- (126) Pang, J.; Yang, Q.; Ma, X.; Wang, L.; Tan, C.; Xiong, D.; Ye, H.; Chen, X. DFT Coupled with NEGF Study of Ultra-Sensitive HCN and HNC Gases Detection and Distinct I – V Response Based on Phosphorene. *Physical Chemistry Chemical Physics* **2017**, *19* (45), 30852–30860.
- (127) Qin, X.; Yan, W.; Li, D.; Zhang, Z.; Chen, S. A First-Principles Study of Gas Molecule Adsorption on Carbon-, Nitrogen-, and Oxygen-Doped Two-Dimensional Borophene. *Advances in Condensed Matter Physics* **2021**, *2021*.
- (128) Huo, Y.; Liu, R.; Sun, Q.; Yang, Z.; Xu, L. C.; Liu, X. Inorganic Gas Sensing Performance of X₃-Borophene and the van Der Waals Heterostructure. *Appl Surf Sci* **2022**, *581*, 151906.
- (129) Phuong, L. T. T.; Phong, T. C. Tuning the Electronic Heat Capacity and Thermal Schottky Anomaly of Monolayer B₁₂-Borophene via Adsorbed Gas Molecules. *Physica E Low Dimens Syst Nanostruct* **2024**, *156*, 115857.
- (130) Hossain, M. A.; Hossain, M. R.; Hossain, M. K.; Khandaker, J. I.; Ahmed, F.; Ferdous, T.; Hossain, M. A. An Ab Initio Study of the B₃₅ Boron Nanocluster for Application as Atmospheric Gas (NO, NO₂, N₂O, NH₃) Sensor. *Chem Phys Lett* **2020**, *754*, 137701.
- (131) Martinez-Gutierrez, G.; Alvarado-Leal, L. A.; Paez-Ornelas, J. I.; Quijano-Briones, J. J.; Ponce-Perez, R.; Fernandez-Escamilla, H. N.; Guerrero-Sanchez, J.; Perez-Tijerina, E. G. Adsorption and Inactivation of Pollutant Molecules on the Hexagonal Borophene/Al(111) Superstructure. *Surfaces and Interfaces* **2024**, *44*, 103730.
- (132) Sabokdast, S.; Salami, N. Prediction of Gas Adsorption on X₃ Borophene: A Density Functional Theory Study. *Solid State Commun* **2023**, *368*, 115174.
- (133) Zhang, J.; Liu, X.; Neri, G.; Pinna, N. Nanostructured Materials for Room-Temperature Gas Sensors. *Advanced Materials* **2016**, *28* (5), 795–831.
- (134) Cui, J.; Shi, L.; Xie, T.; Wang, D.; Lin, Y. UV-Light Illumination Room Temperature HCHO Gas-Sensing Mechanism of ZnO with Different Nanostructures. *Sens Actuators B Chem* **2016**, *227*, 220–226.
- (135) Schedin, F.; Geim, A. K.; Morozov, S. V.; Hill, E. W.; Blake, P.; Katsnelson, M. I.; Novoselov, K. S. Detection of Individual Gas Molecules Adsorbed on Graphene. *Nat Mater* **2007**, *6* (9), 652–655.
- (136) Hieu, N. N.; Tho, T. T.; Bau, N. Q.; Hoi, B. D. Probing Pauli Susceptibility of B₁₂-Borophene in the Presence of Gas Molecules. *J Magn Magn Mater* **2024**, *590*, 171697.
- (137) Zergani, F.; Tavangar, Z. Gas Sensing Behavior and Adsorption Mechanism on X₃ Borophene Surface. *Chemical Engineering Journal* **2022**, *431*, 133947.
- (138) Dutta, N.; Devi, R.; Boruah, A.; Acharjee, S. Analytic Modelling of Quantum Capacitance and Carrier Concentration for B₁₂-Borophene FET Based Gas Sensor. *Physica B Condens Matter* **2023**, *669*, 415262.

- (139) Padilha, J. E.; Miwa, R. H.; Fazzio, A. Directional Dependence of the Electronic and Transport Properties of 2D Borophene and Borophane. *Physical Chemistry Chemical Physics* **2016**, *18* (36), 25491–25496.
- (140) Yu, Z.; Li, Y.; Yu, X.; Chen, F. Computational Study of Borophene with Line Defects as Sensors for Nitrogen-Containing Gas Molecules. *ACS Appl Nano Mater* **2020**, *3* (10), 9961–9968.
- (141) Hembram, K. P. S. S.; Park, J.; Lee, J. K. Unraveling the Mechanism of Doping Borophene. *ChemistryOpen* **2024**, *13* (3), e202300121.
- (142) Li, Z.; Guan, X.; Pandey, G.; Chahal, S.; Bandyopadhyay, A.; Awasthi, K.; Kumar, P.; Vinu, A. Microwave Doping of Sulfur and Iron in B12 Borophene. *Small* **2024**, 2307610.
- (143) Zhang, C.; He, Q.; Chu, W.; Zhao, Y. Transition Metals Doped Borophene-Graphene Heterostructure for Robust Polysulfide Anchoring: A First Principle Study. *Appl Surf Sci* **2020**, *534*, 147575.
- (144) Yang, F.; Song, P.; Ruan, M.; Xu, W. Recent Progress in Two-Dimensional Nanomaterials: Synthesis, Engineering, and Applications. *FlatChem* **2019**, *18*, 100133.
- (145) Hassani, N.; Mehdizade, M. Exploring the Adsorption and Sensing Behavior of the M-Nx-B36-x (M=Fe, Ni, and Cu; X=0, 3) Bowl-Shaped Structures upon CO, NO, O2, and N2 Molecules: A First-Principles Study. *Physica E Low Dimens Syst Nanostruct* **2020**, *124*, 114242.
- (146) Kumar, S.; Singh, M.; Sharma, D. K.; Auluck, S. Enhancing Gas Adsorption Properties of Borophene by Embedding Transition Metals. *Computational Condensed Matter* **2020**, *22*, e00436.
- (147) Anversa, J.; Baierle, R. J.; Rupp, C. J. Hazardous (NO2, NO, CO, CO2, SO2, and NH3) Molecules Interacting with Pt-Decorated B12 Borophene. A First-Principle Study. *Surf Sci* **2023**, *738*, 122370.
- (148) Khan, M. I.; Aziz, S. H.; Majid, A.; Rizwan, M. Computational Study of Borophene/Boron Nitride (B/BN) Interface as a Promising Gas Sensor for Industrial Affiliated Gasses. *Physica E Low Dimens Syst Nanostruct* **2021**, *130*, 114692.
- (149) Li, J.; Chen, X.; Yang, Z.; Liu, X.; Zhang, X. Highly Anisotropic Gas Sensing of Atom-Thin Borophene: A First-Principles Study. *J Mater Chem C Mater* **2021**, *9* (3), 1069–1076.
- (150) Tian, Y.; Yang, H.; Li, J.; Hu, S.; Cao, S.; Ren, W.; Wang, Y. A Comprehensive First-Principle Study of Borophene-Based Nano Gas Sensor with Gold Electrodes. *Front Phys* **2021**, *17* (1).
- (151) Shahbazi Kootenaei, A.; Ansari, G. B36 Borophene as an Electronic Sensor for Formaldehyde: Quantum Chemical Analysis. *Phys Lett A* **2016**, *380* (34), 2664–2668.
- (152) Wang, C. B.; Lu, Q.; Zhang, L. L.; Xu, T. T.; Gong, W. J. Li-Decorated Borophene-Graphene Heterostructure under Gas Adsorption. *Journal of Physics and Chemistry of Solids* **2022**, *171*, 111033.
- (153) Lin, B.; Dong, H.; Du, C.; Hou, T.; Lin, H.; Li, Y. B40 Fullerene as a Highly Sensitive Molecular Device for NH3 Detection at Low Bias: A First-Principles Study. *Nanotechnology* **2016**, *27* (7), 075501.
- (154) Fazilaty, M.; Pourahmadi, M.; Reza Shayesteh, M.; Hashemian, S. X3-Borophene-Based Detection of Hydrogen Sulfide via Gas Nanosensors. *Chem Phys Lett* **2020**, *741*, 137066.
- (155) Arkoti, N. K.; Pal, K. Improved Selectivity of Borophene Sensor towards NO2 Gas with PEI-ZIF-8 Overlayer. *Sens Actuators B Chem* **2024**, *401*, 135033.
- (156) Murugesan, B.; kumar Chinnalagu, D.; Rajaiah, A.; Dai, J.; Dong, Y.; Li, N.; Mahalingam, S.; Cai, Y. Integration of 2D Borophene into Semiconducting N, P, S, and F-Doped 1D Carbon for Energy Storage and Conversion Devices. *Chemical Engineering Journal* **2024**, *499*, 156619.
- (157) Le, P. T. T.; Phong, T. C.; Yarmohammadi, M. B12-Borophene Becomes a Semiconductor and Semimetal via a Perpendicular Electric Field and Dilute Charged Impurity. *Physical Chemistry Chemical Physics* **2019**, *21* (39), 21790–21797.
- (158) Arkoti, N. K.; Pal, K. Work Function Modification of Borophene by Barium Decoration Towards Room Temperature NO2 Gas Sensor. *Proceedings of IEEE Sensors* **2022**, 2022-October.
- (159) Jha, R. K.; Nanda, A.; Bhat, N. Boron Nanostructures Obtained via Ultrasonic Irradiation for High Performance Chemiresistive Methane Sensors. *Nanoscale Adv* **2020**, *2* (5), 1837–1842.
- (160) Hou, C.; Tai, G.; Liu, Y.; Liu, X. Borophene Gas Sensor. *Nano Res* **2022**, *15* (3), 2537–2544.
- (161) Hou, C.; Tai, G.; Liu, B.; Wu, Z.; Yin, Y. Borophene-Graphene Heterostructure: Preparation and Ultrasensitive Humidity Sensing. *Nano Res* **2021**, *14* (7), 2337–2344.
- (162) Hou, C.; Tai, G.; Liu, Y.; Wu, Z.; Liang, X. Ultrasensitive Humidity Sensing and the Multifunctional Applications of Borophene-MoS2 Heterostructures. *J Mater Chem A Mater* **2021**, *9* (22), 13100–13108.
- (163) Mishra, R. K.; Sarkar, J.; Verma, K.; Chianella, I.; Goel, S.; Nezhad, H. Y. Borophene: A 2D Wonder Shaping the Future of Nanotechnology and Materials Science. *Nano Materials Science* **2024**.
- (164) Kumar, S.; Kushwaha, C. S.; Singh, P.; Kanojia, K.; Shukla, S. K. Chemiresistive Sensor for Breath Frequency and Ammonia Concentration in Exhaled Gas over a PVA/PANI/CC Composite Film. *Sensors & Diagnostics* **2023**, *2* (5), 1256–1266.
- (165) Lherbier, A.; Rafael Botello-Méndez, A.; Charlier, J. C. Electronic and Optical Properties of Pristine and Oxidized Borophene. *2d Mater* **2016**, *3* (4), 045006.
- (166) Guo, R. Y.; Li, T.; Shi, S. E.; Li, T. H. Oxygen Defects Formation and Optical Identification in Monolayer Borophene. *Mater Chem Phys* **2017**, *198*, 346–353.
- (167) Moddemann, W. E.; Burke, A. R.; Bowling, W. C.; Foose, D. S. Surface Oxides of Boron and B12O2 as Determined by XPS. *Surface and Interface Analysis* **1989**, *14* (5), 224–232.
- (168) Bi, T.; Zhang, J.; Wang, M.; Wang, L.; Chen, J.; Hu, S.; Chen, C.; Wang, H. Nickel Foam Deposited with Borophene Sheets Used as a Self-Supporting Binder-Free Anode for Lithium-Ion Batteries. *CrystEngComm* **2023**, *25* (23), 3391–3402.
- (169) Wang, H.; An, D.; Wang, M.; Sun, L.; Li, Y.; Li, H.; Li, N.; Hu, S.; He, Y. B. Crystalline Borophene Quantum Dots and Their Derivative Boron Nanospheres. *Mater Adv* **2021**, *2* (10), 3269–3273.
- (170) Wu, Z.; Shifan, C.; Wu, Z.; Liu, Y.; Shao, W.; Liang, X.; Hou, C.; Tai, G. Epitaxial Growth of Borophene on Graphene Surface towards Efficient and Broadband Photodetector. *Nano Res* **2024**, *17* (4), 3053–3060.
- (171) Gu, Q.; Lin, H.; Si, C.; Wang, Z.; Wang, A.; Liu, F.; Li, B.; Yang, B. Tuning the Active Oxygen Species of Two-Dimensional Borophene Oxide toward Advanced Metal-Free Catalysis. *ACS Nano* **2024**.
- (172) Ong, C. W.; Huang, H.; Zheng, B.; Kwok, R. W. M.; Hui, Y. Y.; Lau, W. M. X-Ray Photoemission Spectroscopy of Nonmetallic Materials: Electronic Structures of Boron and BxOy. *J Appl Phys* **2004**, *95* (7), 3527–3534.

- (173) Zeng, X.; Jing, Y.; Gao, S.; Zhang, W.; Zhang, Y.; Liu, H.; Liang, C.; Ji, C.; Rao, Y.; Wu, J.; Wang, B.; Yao, Y.; Yang, S. Hydrogenated Borophene Enabled Synthesis of Multielement Intermetallic Catalysts. *Nat Commun* **2023**, *14* (1), 1–11.
- (174) Li, Q.; Kolluru, V. S. C.; Rahn, M. S.; Schwenker, E.; Li, S.; Hennig, R. G.; Darancet, P.; Chan, M. K. Y.; Hersam, M. C. Synthesis of Borophane Polymorphs through Hydrogenation of Borophene. *Science* **2021**, *371* (6534), 1143–1148.
- (175) Liu, Y.; Tai, G.; Hou, C.; Wu, Z.; Liang, X. Chemical Vapor Deposition Growth of Few-Layer B12-Borophane on Copper Foils toward Broadband Photodetection. *ACS Appl Mater Interfaces* **2023**.
- (176) Wang, Z.; Lü, T. Y.; Wang, H. Q.; Feng, Y. P.; Zheng, J. C. New Crystal Structure Prediction of Fully Hydrogenated Borophene by First Principles Calculations. *Sci Rep* **2017**, *7* (1), 1–11.
- (177) Mozvashi, S. M.; Mohebpour, M. A.; Vishkayi, S. I.; Tagani, M. B. Mechanical Strength and Flexibility in -4H Borophene. *Sci Rep* **2021**, *11* (1), 1–9.
- (178) Rezvani, S. J.; Abdi, Y.; Parmar, R.; Paparoni, F.; Antonini, S.; Gunnella, R.; Di Cicco, A.; Amati, M.; Gregoratti, L.; Mazaheer, A.; Hajibaba, S. Aluminum-Activated Borophene Nanosheets with Enhanced Oxidation Resistance for Nanoelectronic Devices. *ACS Appl Nano Mater* **2024**, *7* (11), 13712–13719.
- (179) Recent, Y.; Kulinich, S.; Wang, Y.; Zhou, Y. Recent Progress on Anti-Humidity Strategies of Chemiresistive Gas Sensors. *Materials* **2022**, *15* (24), 8728.
- (180) Rathi, K.; Pal, K. Wireless Hand-Held Device Based on Polylactic Acid-Protected, Highly Stable, CTAB-Functionalized Phosphorene for CO₂ Gas Sensing. *ACS Appl Mater Interfaces* **2020**, *12* (34), 38365–38375.
- (181) Ko, G. J.; Han, S. D.; Kim, J. K.; Zhu, J.; Han, W. B.; Chung, J.; Yang, S. M.; Cheng, H.; Kim, D. H.; Kang, C. Y.; Hwang, S. W. Biodegradable, Flexible Silicon Nanomembrane-Based NO_x Gas Sensor System with Record-High Performance for Transient Environmental Monitors and Medical Implants. *NPG Asia Mater* **2020**, *12* (1), 1–9.
- (182) Yang, L.; Zheng, G.; Cao, Y.; Meng, C.; Li, Y.; Ji, H.; Chen, X.; Niu, G.; Yan, J.; Xue, Y.; Cheng, H. Moisture-Resistant, Stretchable NO_x Gas Sensors Based on Laser-Induced Graphene for Environmental Monitoring and Breath Analysis. *Microsyst Nanoeng* **2022**, *8* (1), 1–12.
- (183) Gong, K.; Hu, J.; Cui, N.; Xue, Y.; Li, L.; Long, G.; Lin, S. The Roles of Graphene and Its Derivatives in Perovskite Solar Cells: A Review. *Mater Des* **2021**, *211*, 110170.
- (184) Casanova-Chafer, J.; Garcia-Aboal, R.; Llobet, E.; Atienzar, P. Enhanced CO₂ Sensing by Oxygen Plasma-Treated Perovskite-Graphene Nanocomposites. *ACS Sens* **2024**, *9* (2), 830–839.
- (185) Liu, X.; Hersam, M. C. Borophene-Graphene Heterostructures. *Sci Adv* **2019**, *5* (10), 6444–6455.
- (186) Wang, C. B.; Tian, Y. P.; Duan, J. X.; Zhang, B. Y.; Gong, W. J. Enhanced Organic Gas Sensing Performance of Borophene/Graphene van Der Waals Heterostructures via Transition Metal Doping. *Surfaces and Interfaces* **2023**, *43*, 103544.
- (187) Lipatov, A.; Varezhnikov, A.; Wilson, P.; Sysoev, V.; Kolmakov, A.; Sinitskii, A. Highly Selective Gas Sensor Arrays Based on Thermally Reduced Graphene Oxide. *Nanoscale* **2013**, *5* (12), 5426–5434.
- (188) Ren, W.; Zhao, C.; Niu, G.; Zhuang, Y.; Wang, F. Gas Sensor Array with Pattern Recognition Algorithms for Highly Sensitive and Selective Discrimination of Trimethylamine. *Advanced Intelligent Systems* **2022**, *4* (12), 2200169.
- (189) Lee, J.; Jung, Y.; Sung, S. H.; Lee, G.; Kim, J.; Seong, J.; Shim, Y. S.; Jun, S. C.; Jeon, S. High-Performance Gas Sensor Array for Indoor Air Quality Monitoring: The Role of Au Nanoparticles on WO₃, SnO₂, and NiO-Based Gas Sensors. *J Mater Chem A Mater* **2021**, *9* (2), 1159–1167.
- (190) Kim, J. Y.; Bharath, S. P.; Mirzaei, A.; Kim, S. S.; Kim, H. W. Identification of Gas Mixtures Using Gold-Decorated Metal Oxide Based Sensor Arrays and Neural Networks. *Sens Actuators B Chem* **2023**, *386*, 133767.
- (191) Khan, M. A. H.; Thomson, B.; Debnath, R.; Motayed, A.; Rao, M. V. Nanowire-Based Sensor Array for Detection of Cross-Sensitive Gases Using PCA and Machine Learning Algorithms. *IEEE Sens J* **2020**, *20* (11), 6020–6028.
- (192) Zou, Q.; Itoh, T.; Shin, W.; Sawano, M. Machine-Learning-Assisted Sensor Array for Detecting COVID-19 through Simulated Exhaled Air. *Sens Actuators B Chem* **2024**, *400*, 134883.
- (193) Gozar, A.; Bozovic, I.; Wu, R. Quo Vadis, Borophene? *Nano Today* **2023**, *50*, 101856.

Table 1. Advantages, disadvantages, primary and potential improvements for the main borophene synthesis methods.

Synthesis Method	Advantages	Disadvantages	Main Challenge	Potential improvement
Molecular beam epitaxy (MBE)	1) High purity and crystallinity 2) Precise control over layer growth	1) High cost 2) Limited scalability 3) Production of limited quantities	Ensuring reproducibility device-to-device during the layer transfer	Development of advanced transfer methods to preserve layer quality, and exploration of new substrate materials for enhanced compatibility
Chemical vapor deposition (CVD)	1) Obtention of large surface area borophene 2) Reasonable control over thickness and phase purity	1) High temperature requirements limit substrate choices 2) Variability in gas flow into the chamber impacts reproducibility	Maintaining precise control of parameters for reliable scaling in industrial applications	Innovations in developing low-temperature CVD techniques, uniform gas flow systems, and more specific substrates
Sonochemical exfoliation	1) Easily scalable 2) Cost effectiveness	1) Limited control over layer quality 2) Induced structural defects	High density defect accelerates the superficial oxidation processes	Optimization of solvent selection and centrifugation parameters to reduce defects, alongside passivation strategies to address oxidation and stability

Table 2. Theoretical adsorption energies and charge transfer of different electron-withdrawing compounds adsorbed on borophene surface. Selected representative examples are provided for illustration.

Nanomaterial	Electron acceptor gas	Type of adsorption	Adsorption energy (eV)	Charge transfer (e)
Pure borophene ⁵³	NO ₂	Chemisorbed	-2.32	-0.72
MoS ₂ / borophene ¹¹⁴	NO ₂	Chemisorbed	-2.12	-0.80
Pure borophene ⁵³	NO	Chemisorbed	-1.79	-0.62

MoS ₂ / borophene ¹¹⁴	NO	Chemisorbed	-1.47	-1.24
Pure borophene ⁵³	CO ₂	Physisorbed	-0.36	-0.09
MoS ₂ / borophene ¹¹⁴	CO ₂	Physisorbed	-0.64	-0.04
Na-doped borophene ¹¹⁵	CO ₂	Chemisorbed	-0.87	-0.17
Pure borophene ¹¹⁶	SO ₂	Physisorbed	-0.49	-0.09
Li-doped borophene ¹¹⁶	SO ₂	Chemisorbed	-1.36	-0.34
Pure borophene ⁵³	CO	Chemisorbed	-1.38	-0.39
MoS ₂ / borophene ¹¹⁴	CO	Chemisorbed	-1.15	-0.41
Pure borophene ¹¹⁷	HCHO	Chemisorbed	-1.21	-0.32
2H-MoS ₂ / borophene ¹¹⁸	HCHO	Chemisorbed	-2.57	-1.28

Table 3. Theoretical adsorption energies and charge transfer of different electron donor compounds adsorbed on borophene surface. Selected representative examples are provided for illustration.

Nanomaterial	Electron donor gas	Type of adsorption	Adsorption energy (eV)	Charge transfer (e)
Pure borophene ⁵³	NH ₃	Chemisorbed	-1.75	+0.18
Pure borophene ¹¹⁹	HCN	Chemisorbed	-0.65	+0.23
Pure borophene ¹²⁰	CH ₄	Physisorbed	-0.79	+0.01
Graphene/ Borophene ¹²¹	CH ₄	Physisorbed	-0.13	+0.01
2H-MoS ₂ / borophene ¹¹⁸	CH ₄	Physisorbed	-0.17	+0.01
Pure borophene ¹²⁰	CH ₃ OH	Physisorbed	-0.89	+0.02
Graphene/ Borophene ¹²¹	CH ₃ OH	Physisorbed	-0.26	+0.01

2H-MoS ₂ / borophene ¹¹⁸	CH ₃ OH	Physiosorbed	-0.41	+0.01
Pure borophene ¹¹⁷	C ₂ H ₆	Physiosorbed	-0.27	+0.01
Pure borophene ¹²⁰	C ₆ H ₆	Physiosorbed	-0.97	+0.01
Graphene/ Borophene ¹²¹	C ₂ H ₄	Physiosorbed	-0.19	+0.01
2H-MoS ₂ / borophene ¹¹⁸	C ₂ H ₄	Physiosorbed	-0.32	+0.01
Graphene/ Borophene ¹²¹	C ₂ H ₂	Physiosorbed	-0.14	+0.01
SnO ₂ / borophene ¹²²	HCHO	Chemisorbed	-1.81	+0.09
Pure borophene ¹¹⁷	H ₃ CCl	Physiosorbed	-0.29	+0.01

Table 4. Comparison of the sensing performance of published experimental studies that reported borophene-based gas sensors. All sensors were operated under ambient temperature conditions.

Sample	Synthesis method of borophene	Analyte	Response (%) / concentration (ppm)	Response / recovery times (s)
Barium decorated borophene ¹⁵⁸	Sonochemical	NO ₂	51.5 / 25	40 / 44
Borophene-PEI-ZIF-8 ¹⁵⁵	Sonochemical	NO ₂	24.1 / 25	72 / 48
Borophene ¹⁵⁹	Sonochemical	CH ₄	43.5 / 50	42 / 40
Borophene ¹⁶⁰	CVD	NO ₂	422 / 100	30 / 200
Borophene-graphene ¹⁶¹	CVD	H ₂ O	4200 / 80 (% of RH)	10.5 / 8.3
Borophene-MoS ₂ ¹⁶²	CVD	H ₂ O	15500 / 97 (% of RH)	2.5 / 3.1

Table 5. Comparison of XPS characterization of borophene. It is worth noting that significant contents of C and O are observed in experimental studies.

Method	Atomic ratio (at. %)						
	B	C	O	N	Ni	Na	Cu
Sonochemical exfoliation, DMF ⁹⁰	54.6	30.5	12.3	2.6	-	-	-
Sonochemical exfoliation, acetone ⁹⁵	48.72	25.14	25.47	0.67	-	-	-
CVD ¹⁶⁸	40.56	9.67	48.77	-	1.06	-	-
Sonochemical exfoliation, IPA ¹⁶⁹	27.28	13.04	57.7	1.99	-	-	-
CVD ⁸⁶	17.3	71.69	9.35	0.94	-	0.73	-
CVD ¹⁷⁰	32.94	34.49	10.49	-	-	1.61	17.84

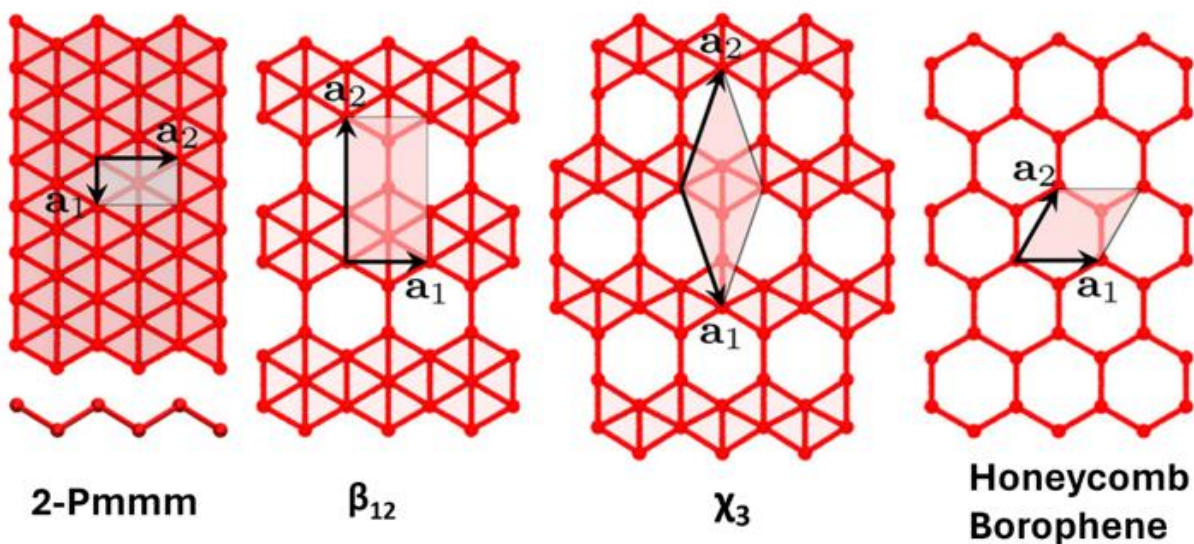


Figure 1. The most studied 2D-borophene phases: 2-*Pmmn*, β_{12} , χ_3 , and honeycomb borophene. The terms a_1 and a_2 represent the lattice vectors. Reproduced from 63. Copyright 2016, American Chemical Society.

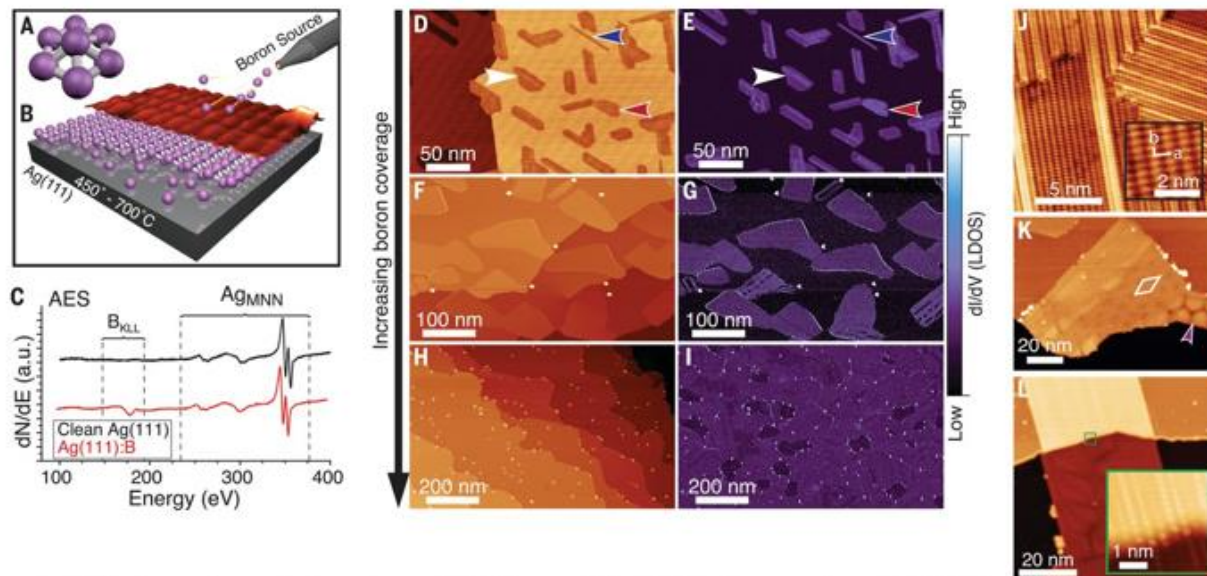


Figure 2. (a) B₇ borophene cluster phase. (b) Scheme of the MBE setup employed. (c) AES spectra of bare Ag (111) substrate before and after borophene deposition. (d-i) STM topography (left) and closed-loop dI/dV (right) at different magnifications. (j-l) STM topography images of rectangular lattice (top), Rhombohedral and honeycomb phases (middle), and carpet-mode growth (bottom). Reproduced from 48. Copyright 2015, American Association for the Advancement of Science (AAAS).

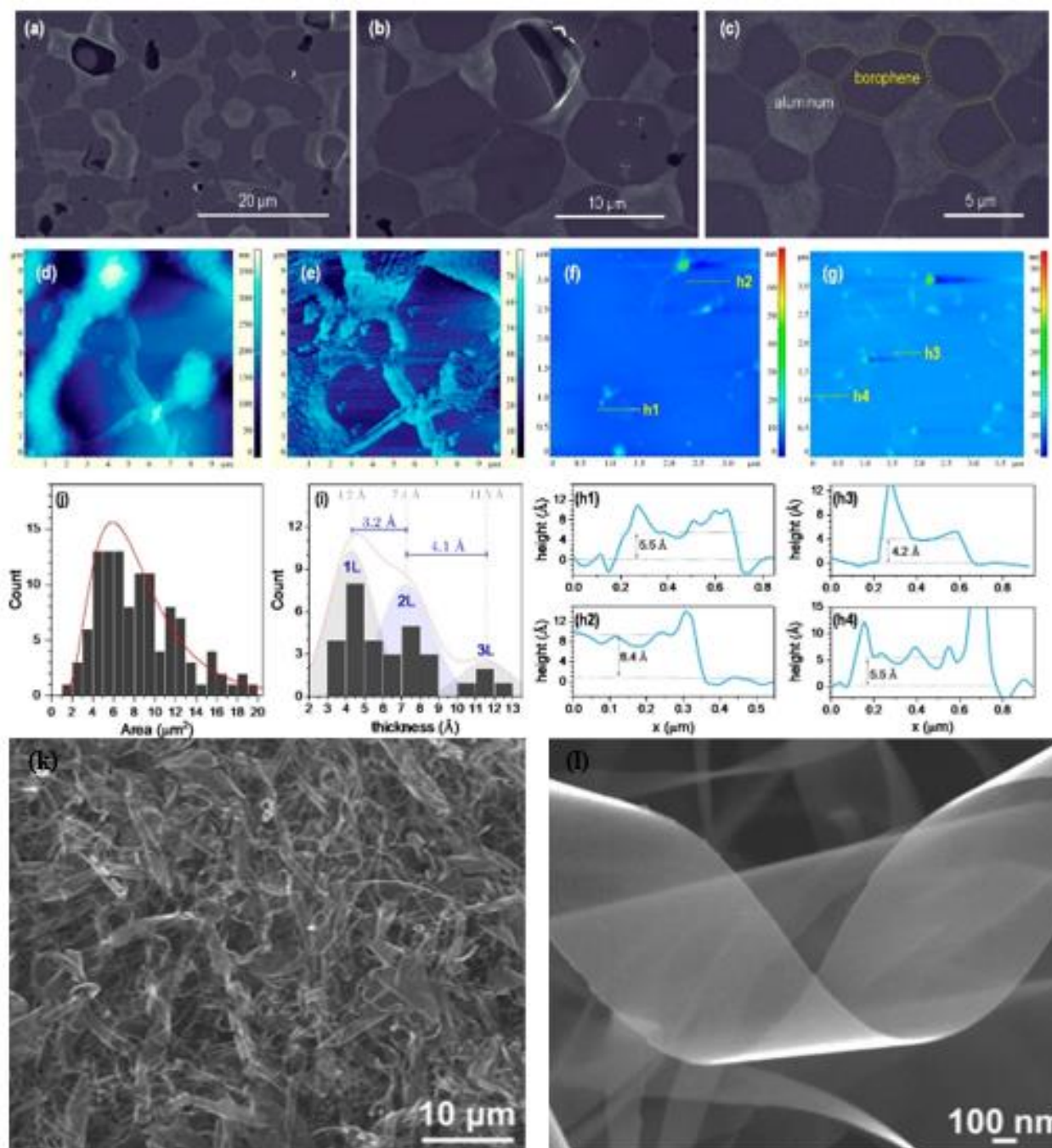


Figure 3. Borophene obtained via the CVD method. (a–c) SEM images of borophene (gray regions) and aluminum (bright areas) corresponding to the metal substrate. (d, e) Borophene AFM images and their corresponding phase diagram (f, g). Area (i) and thickness (j) of boron sheets. (h1–h4) Thickness profiles of different layers. Reproduced from permission 83. Copyright 2021, American Chemical Society. (k–l) SEM images depict single-crystalline ultrathin borophene obtained via CVD. (k) At lower magnification, this image reveals the enlarged diameter of the boron sheets at the micrometer scale. In contrast, in (l), the higher magnification image demonstrates the ultra-low thickness achieved. Reproduced from 84. Available under CC BY 4.0 license. Copyright 2015, Wiley.

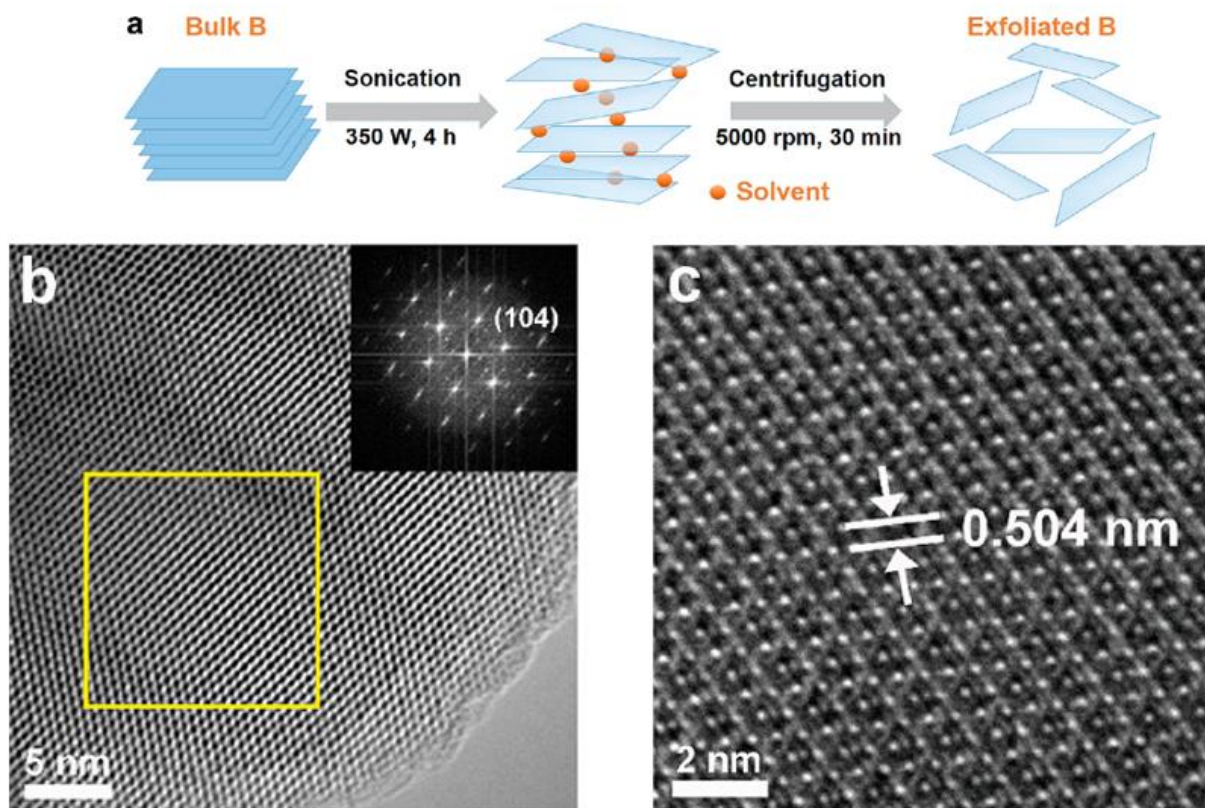


Figure 4. (a) Schematic representation of sonochemical exfoliation. The sonication promotes the intercalation of solvent molecules between the bulk boron sheets, followed by centrifugation-induced exfoliation. (b-c) Transmission electron microscope (TEM) images demonstrate that this method enables the production of nano-sized borophene with high crystallinity. Reproduced from 90. Copyright 2018, American Chemical Society.

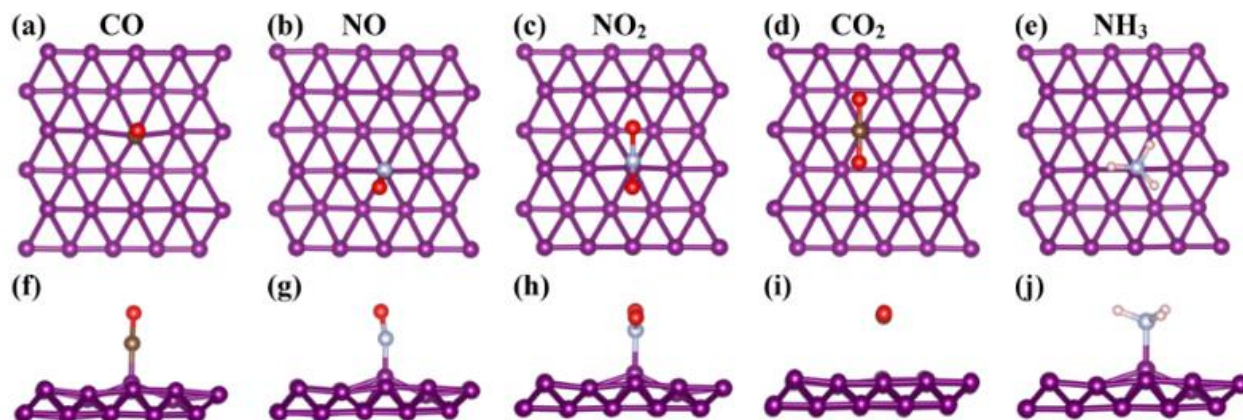


Figure 5. (a-g) top and (f-j) side perspectives of the relaxed structures of a borophene monolayer with adsorbed gases CO, NO, NO₂, CO₂, and NH₃. Purple balls represent boron atoms, while nitrogen (N), oxygen (O), hydrogen (H), and carbon (C) atoms are denoted by gray, red, pink, and brown balls, respectively. Reproduced from 53. Copyright 2017, American Chemical Society.

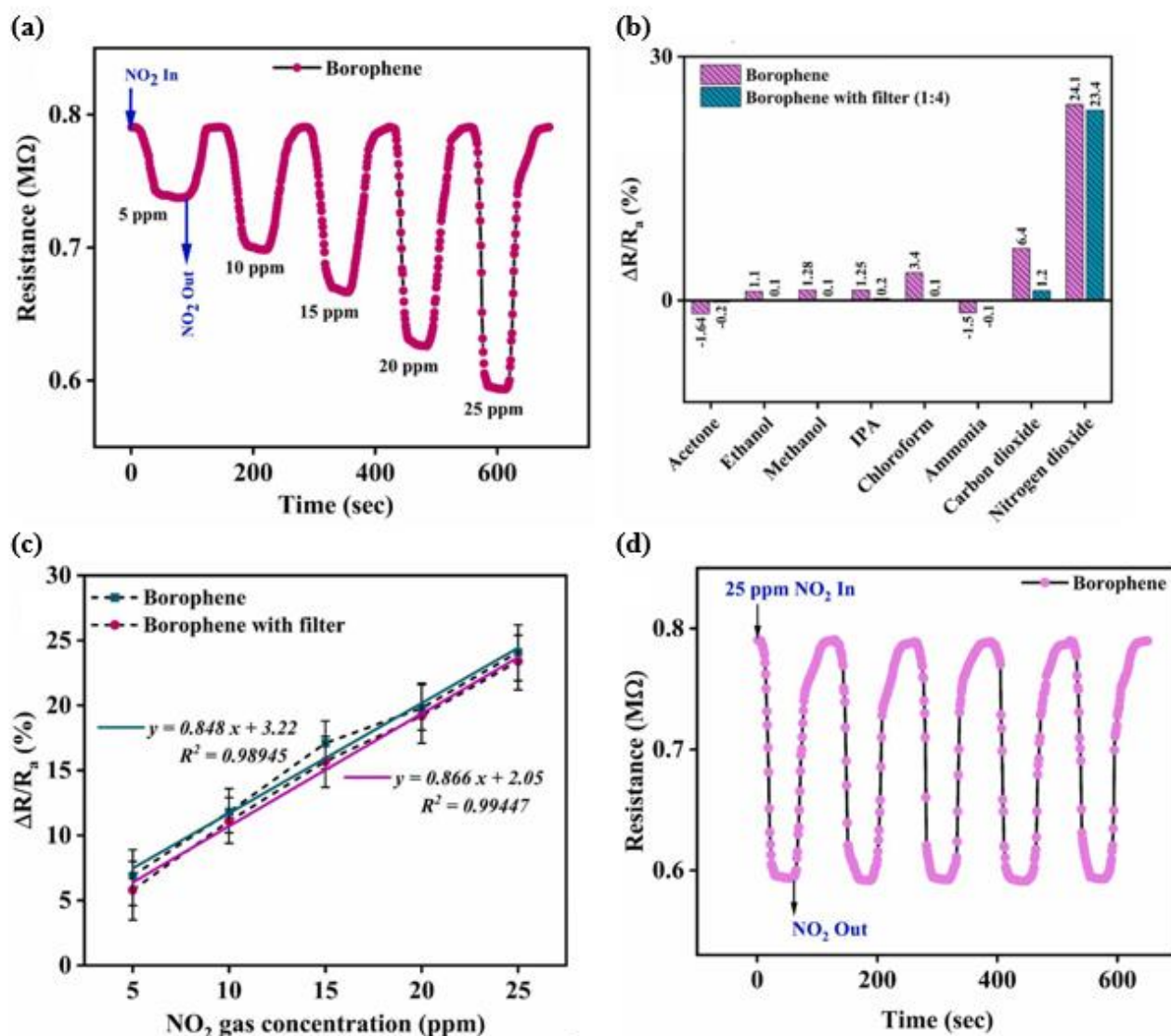


Figure 6. (a) Example of the electrical responses obtained for detecting five concentrations of NO₂ at RT and 35% RH employing a borophene sensor. (b) Comparison of the NO₂ sensing performance employing borophene with and without a selective filter for NO₂. It can be observed that the sensitivity towards other gases significantly decreases when using a filter, while the NO₂ response is only slightly affected. (c) Calibration curves for NO₂ detection under the same experimental conditions. No significant changes in the regression are observed, indicating that using a selective filter does not jeopardize the NO₂ detection. (d) Example of the borophene repeatability towards 25 ppm of NO₂. Reproduced from 155. Copyright 2024, Elsevier.

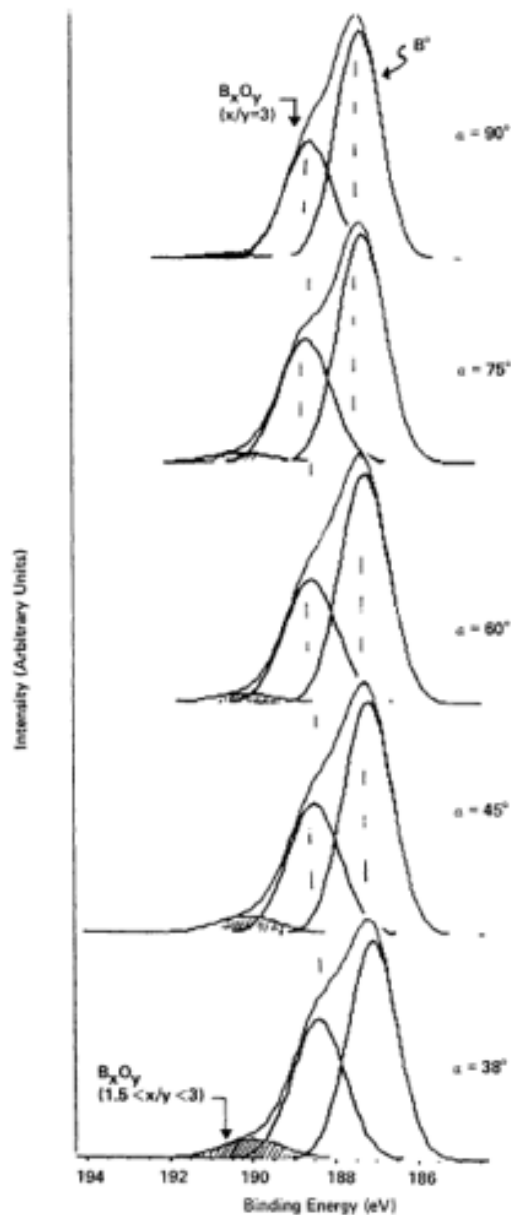


Figure 7. Boron 1s XPS spectra recorded at different take-off angles (α). Three main peaks are observed after deconvolution: B^0 , corresponding to B-B bonds, and two B_xO_y peaks associated with a suboxide layer. XPS spectra were recorded at take-off angles ranging from 90° to 38° . As the take-off angle decreases, photoelectrons from increasingly superficial layers are detected. Consequently, the greater prominence of suboxide peaks at lower take-off angles indicates that boron oxidation is predominantly confined to the surface. Reproduced from 167. Copyright 1989, Wiley.

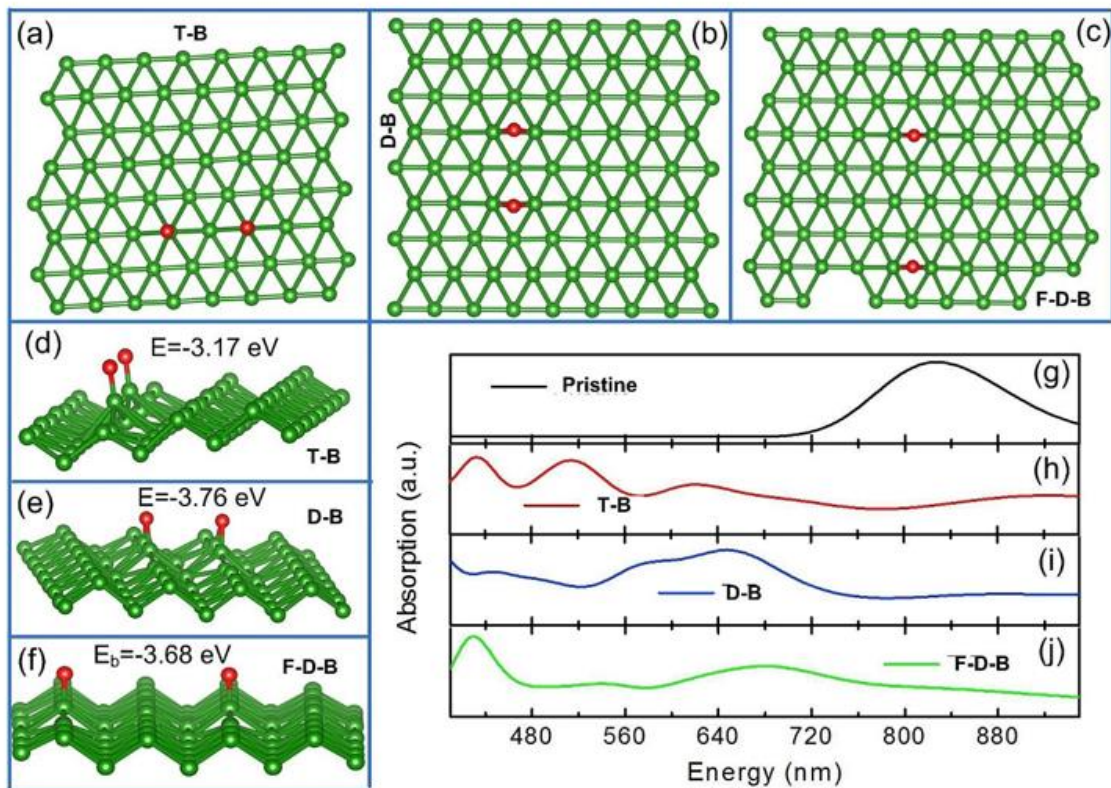


Figure 8. (a) - (c) Top view of borophene (boron atoms represented as green dots) with two possible chemisorbed oxygen atoms (red dots). T-B: smallest binding energy. D-B: largest binding energy. F-D-B: interaction between dangling oxygen atoms depending on the distance and the relative position of B-O. (d) - (f) Side view of chemisorbed oxygen on borophene surface. (g) - (j) Adsorption spectra for the different configurations of oxygen chemisorption on borophene. Reproduced from 166. Copyright 2017, Elsevier.

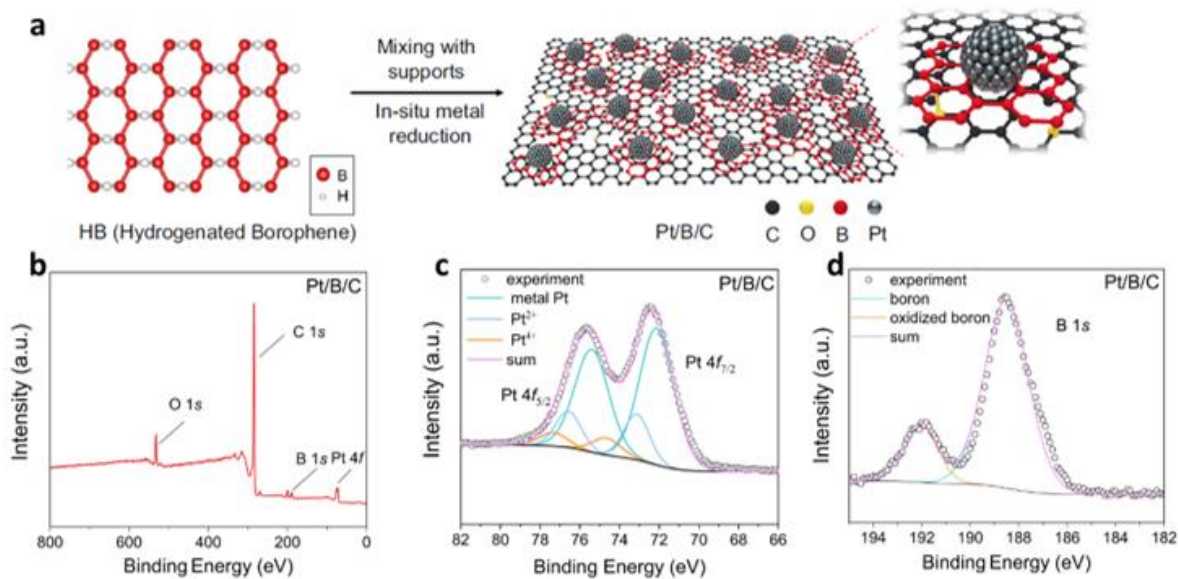


Figure 9. (a) Scheme of the borophene supported on a carbon support and decorated with platinum nanoparticles, (b) XPS survey spectra of the Pt/B/C sample, (c) deconvolution of Pt 4f peak, and (d) deconvolution of the B 1s peak. Reproduced from 173. Available under CC BY 4.0 license. Copyright 2023, Nature.